

2001

Investigation of fluvial responses to natural variations in discharge and sediment yield : insights from a supply-limited system in a glacierized basin

Justin Thomas Pearce
Lehigh University

Follow this and additional works at: <http://preserve.lehigh.edu/etd>

Recommended Citation

Pearce, Justin Thomas, "Investigation of fluvial responses to natural variations in discharge and sediment yield : insights from a supply-limited system in a glacierized basin" (2001). *Theses and Dissertations*. Paper 700.

This Thesis is brought to you for free and open access by Lehigh Preserve. It has been accepted for inclusion in Theses and Dissertations by an authorized administrator of Lehigh Preserve. For more information, please contact preserve@lehigh.edu.

Pearce, Justin
Thomas

INVESTIGATIONS
OF FLUVIAL
RESPONSES TO
NATURAL
VARIATIONS IN
DISCHARGE...

June 2001

Investigations of fluvial responses to natural variations in discharge and sediment

yield: Insights from a supply-limited system in a glacierized basin

By

Justin Thomas Pearce

A Thesis

Presented to the Graduate and Research Committee

Of Lehigh University

In Candidacy for the Degree of

Master of Science

In

Geological Sciences

Lehigh University

May 4, 2001

JUSTIN T. PEARCE THESIS SIGNATURE SHEET

This thesis is accepted and approved in fulfillment of the requirements for the
Master of Science degree.

April 26th 2001
Date

Dr Frank J. Pazzaglia
Thesis Advisor

Dr Peter K. Zeitler
Department Chairperson

Preface

This following manuscript is the culmination of 80 days of fieldwork at the Matanuska Glacier, Alaska, in the summer of the year 2000. This research opportunity was filled with trial and tribulation, as well as unexpected success and academic growth. When the field season ended, we left with data on such processes as sub-glacial discharge of meltwater and sediment, tributary drainage basin sediment delivery, fluvial response to localized base-level fall and to melt-season variations in sediment and discharge. The author was very fortunate to have had the opportunity to work in such a geologically dynamic field location.

Chapter 1 of this work details the results and interpretations of the data collected for the purpose of quantifying and understanding the relative contribution of coarse bedload to the overall glacial erosion budget. Contrary to our original working hypothesis, this turns out to be negligible portion of the overall sediment yield. The availability of sediment strongly controls the magnitudes of mass fluxed out of the vents. This is quite useful knowledge to have, as supply-limited systems ignore predictive formulae.

Chapter 2 thoroughly examines the extent of impact and fluvial adjustments to changes in base level, discharge, and sediment load. It is found that the system is well graded to the fluctuations in magnitude of discharge and sediment load. In addition,

we document and characterize the pre- syn- and post-baselevel fall conditions of the channel. The results of this analysis show that the system response is characterized by an overall exponential decay curve, with a complex response of alternation between sediment storage and evacuation.

The author has benefited greatly, both personally and professionally, from the creation of this manuscript. It is hoped that the reader will derive insight from this work, and that this knowledge will contribute in some small part to the geologic community.

Acknowledgements

This research was supported in part by Geological Society of America grant number 6763-00, as well as by the US Army Cold Regions Research and Engineering Laboratories. This manuscript benefited from reviews and comments from F.J. Pazzaglia, E.B. Evenson, D.E. Lawson, D. Germanoski, and two anonymous reviewers.

The author would like to acknowledge B. Cashman for valuable creativity and assistance in the field, and F.J. Pazzaglia for unwavering faith and support in the authors abilities, judgement, and interpretations. Also, the author acknowledges the “Matanuska Mafia” for the opportunity to participate and contribute to their overall research in Alaska.

Finally, the author acknowledges those who have, directly or indirectly, contributed to this manuscripts success. There are too many to name individually, but includes my friends and colleagues at Lehigh University and UNM, my family for believing in me, and to my officemate N. (El Ocho) Scala, D. Latta and N. Harkins, for stress relief. Most especially I thank Sarah A. Newland for her unconditional support, encouragement, and laughter when needed.

TABLE OF CONTENTS

Title page	i
Certificate of Approval	ii
Preface	iii
Acknowledgements	v
List of Figures	vii
List of Tables	ix
Chapter 1	1
Chapter 2	29
References	62
Vita	64

List of Figures.

- Figure 1-1. Location map showing Matanuska Glacier and its watershed boundary, Hick's Creek tributary, and the approximate sample locations (open circles). LR is on the west side of the terminus, NV is on the north side. Blowup map is UTM coordinate system, zone 11. 6
- Figure 1-2a. Shows trends in BLF versus SLF in relation to discharge. Dashed line represents generalized flux variation paths, a schematic representation of the system sediment yield behavior. The inset figure plots BLF as a function of discharge. 11
- Figure 1-2b. Shows trends in North Vent BLF versus SLF in relation to discharge. Dashed line represents generalized flux variation paths, a schematic representation of the system sediment yield behavior. The inset figure plots BLF as a function of discharge. 12
- Figure 1-3a. Plot of LR trend in grain size distribution through the melt season. Values shown in legend indicates measured flux values. 13
- Figure 1-3b. Plot of NV trend in grain size distribution through the melt season. Values shown in legend indicates measured flux values. 14
- Figure 2-1. Location map of study area. Open circle is approximate location. The trunk Matanuska River is shown, although it should not be inferred that the LR vent is the sole source of discharge to that river. 30
- Figure 2-2. Little River vent. Vent to channel transition is at the right of the page. Note person for scale, instability of hillslopes, and incision of moraine. Vent bedload sample location is indicated by white arrow. 33
- Figure 2-3. Upstream view of LR showing vegetated and bare bars. Line depicts approximate location of moraine that is breached. Location of picture is approximately 5 m north of (0,0) on Figure 2-5. 35
- Figure 2-4. Littler River hydrograph with bedload flux data. 36

Figure 2-5a. LR early season channel map.	38
Figure 2-5b. LR late season channel map.	39
Figure 2-6a. Little River south bank long-profile comparison.	46
Figure 2-6b. Long profiles and clay ring elevations from backwater area.	47
Figure 2-7. Little River cross section profiles. View is in the downstream direction (see figure 2-5 for location).	49
Figure 2-8. LR bedload rating curve measured at cross section.	53
Figure 2-9. Shows the deposited clastic “wedge” upstream of the culverts. Dashed line is cross section location from Figure 2-5. Flow is from upper right to lower left of page.	57
Figure 2-10. Magnitude of fluvial response through time.	60

List of Tables.

Table 1-1. Bedload sample masses, fluxes, and grain size distributions.	13
Table 2-1. Little River bedload data.	51

Abstract

Magnitudes of glacially derived bedload flux and the relative ratios between the suspended and bedload components of total sediment load are highly debated. Published data indicate large extremes in the ratio between glacially-derived suspended load and bedload, measured from pro-glacial channels. This ratio can range from $< 30\%$ to $> 75\%$ bedload, depending on the specific glacier setting. Two “vents”, which are the sources for supercooled sub-glacial meltwater discharge, were sampled over the course of an entire melt season in order to quantify the flux of glacially delivered bedload at the Matanuska Glacier. The results of the calculations show that the bedload component is negligible and may not be a significant contribution to the total glacier erosion budget. Furthermore, it is revealed that the bedload fluxes are strongly supply-limited, as shown by the poor correlation between discharge and bedload capacity. Thus, in this case, any attempt at employing a predictive quantitative expression for erosion based on discharge alone would be invalid. Analysis of the data is cast in the context of inherent glacial variability (presumably related to the sub-glacial drainage network), as well as implications for erosional styles of a steady-state temperate glacier.

Introduction

No one doubts that glaciers erode; the important questions are how much, how fast, and by what process. Numerical derivations have been put forth to quantitatively describe the ranges and rates of glacial erosional processes (Alley et al, 1997), yet there still remains relatively little field data on which to constrain and base the boundary conditions of these models.

In the context of global denudation, the role of small, mountainous basins has recently been shown to be capable and culpable of delivering a disproportionately high amount of sediment out of the basins than previously thought, when compared to continental-scale drainage basins such as the Amazon, Mississippi, or Ganges-Bramaputra systems (Milliman and Syvitski, 1992; Jaegar, 1998). Moreover, it is also recognized that the ranges and rates of denudation in glaciated basins are significantly higher than those of non-glaciated basins (Hunter, 1996; Hallet et al, 1996). In order to quantify the rates and magnitudes of erosion from glaciated (and non-glacierized) basins, attention must be focussed on the fluvial system, as it is the route through which all sediment must egress.

As glaciers release their entrained sediment to the glacio-fluvial drainage network, there are two components of the total load, the bedload and the suspended load. Because of the relative ease of sampling in the field, the suspended load for

many glaciated basins has been well documented and quantified (Lawson, 1993; Bogen, 1996; Gurnell, 1987). In this light, the geologic community has learned much about the spatio-temporal variation, patterns, and behaviors of glacial suspended sediment delivery and load. However, due to the physical and logistical difficulties of sampling, as well as inherent variability, there is a lack of data pertaining to the amounts and rates of bedload flux through these systems. It then becomes necessary to sample manually for the bedload value, because it could potentially be a large contributor to the overall estimation of the basin-wide erosion rates, and as such needs to be constrained. Available glacial bedload data are compiled and well summarized by Hallet et al (1996), Gurnell and Clark (1987), and others, yet many questions remain. For instance, Bogen (1989) found that over the years 1969 – 1993, the Nigardsbreen glacier bedload vs. suspended load ratio fluctuates stochastically, but averages to 44% bedload. Much continuing debate exists as to what the ratios of suspended load versus bedload actually are in regards to glacial erosion. Specifically, can a representative fraction be employed in estimating erosion, especially considering the uniqueness of independent glacial types, movement conditions, bedrock lithologies, basin climate and hydrology.

At our study area, there are sub-rounded to rounded cobbles in the pro-glacial channels and vent fringes. It is poorly understood whether these clasts are being

delivered to the sub-glacial drainage system via inwash, via physical erosion of the bedrock, whether they are the remnants of fluvial reworking of moraines, or if they are delivered to the terminus by smaller tributary basins.

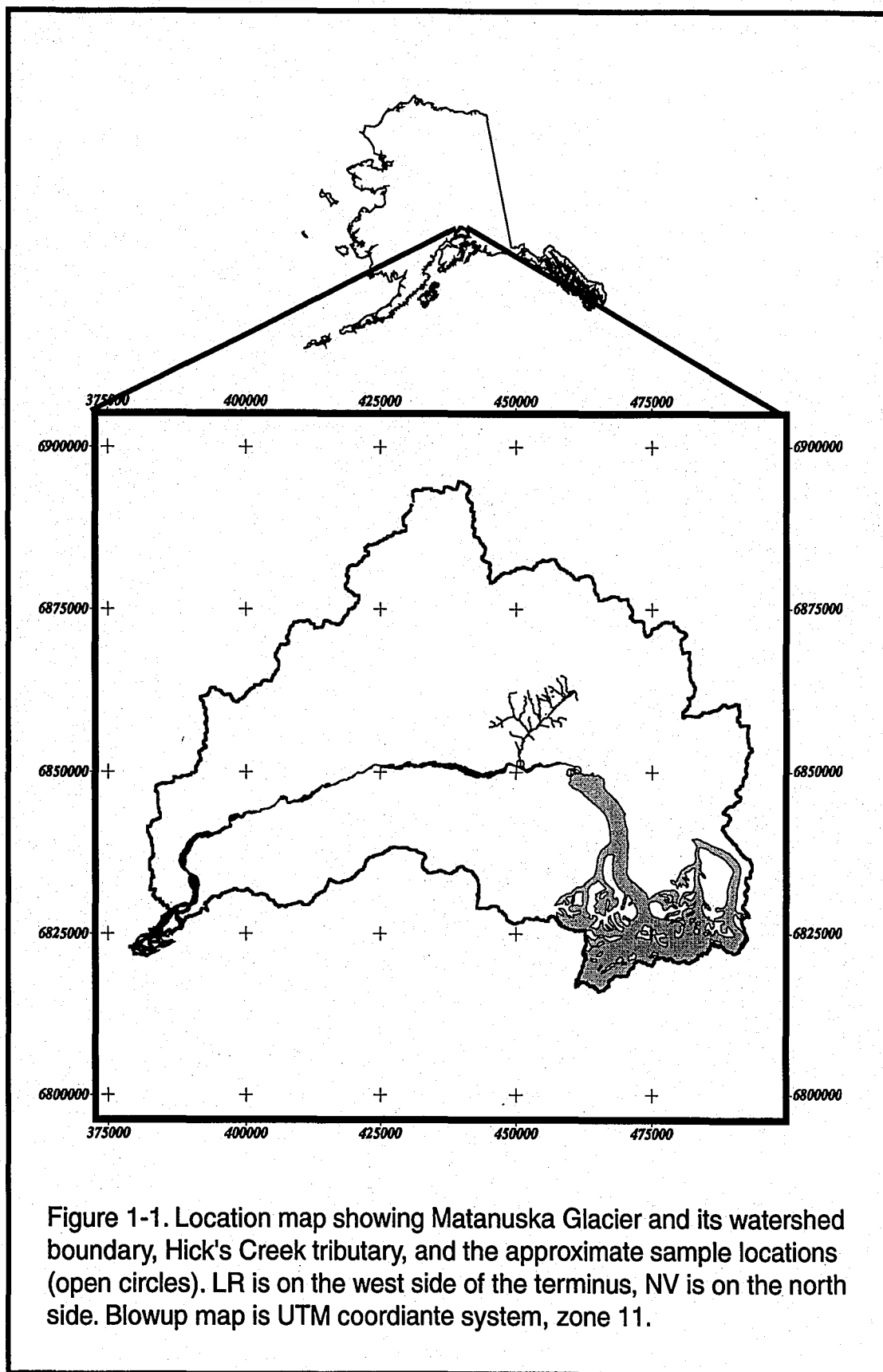
The fluvial systems that drain the Matanuska Glacier in south-central Alaska are uniquely situated to address the question of coarse sediment production. Herein we will present bedload sediment flux data collected from an entire melt season. This data will be compared with suspended sediment load data, as well as data from a non-glaciated tributary basin just downstream of the glacier terminus, in order to provide context regarding the relative evacuation rates between glaciated and non-glaciated basins. A central goal of this paper will be to determine if there is any meaningful predictive relationship between discharge and bedload flux. We will attempt to demonstrate that, in this case, glacially-derived bedload magnitudes are negligibly small, and that the role of smaller, non-glaciated tributary basins to overall flux of sediment, and hence denudation, is larger than expected. Furthermore, we will present plausible and alternative scenarios as to why this is the case.

Physical Setting

The Matanuska Glacier, located 100 miles northeast of Anchorage, Alaska, covers approximately 280 km² in area, and is situated in the east-west trending valley

between the Talkeetna Mountains to the north, and the Chugach Mountains to the south (Figure 1-1). The Matanuska Glacier is classified as a temperate glacier, where liquid and solid phases of water coexist at or below 0°C (Lawson, 1993). In certain places along the glacier terminus, supercooled, sediment-laden, sub-glacial meltwater erupts upward due to hydrostatic pressure and is manifested at the surface as “vents” (Evenson et al, 1999). The load of suspended sediment from these discharge vents has been well quantified over the past few years (Lawson, 1993). In contrast, the bedload component has not been as extensively studied.

The source of meltwater and sediment discharge to the fluvial system is from “vents”, where sub-glacial meltwater is expunged. The vents typically have a lake-like morphology, with the sub-glacial discharge appearing as a 1-meter fountain in the middle of the body of water when hydrostatic pressure builds up. Two such vents were chosen for sampling during the summer 2000 melt season, the North Vent (NV) and Little River (LR). These vents were selected primarily because of their accessibility and flow wade-ability. The Little River vent is situated behind a moraine, and has hillslopes of vegetation-free, debris-covered ice. The ice melts as the summer progresses, instigating many small-scale mudflows. These mudflows, referred to as “inwash”, are a dominant process for delivering coarse and fine sediment to the fluvial system. The North Vent, in contrast, has a thick cover of



vegetation binding the surrounding ice-cored hillslopes, and therefore receives little to no inwash during the melt season.

Methods

Bedload data was collected using two Helley-Smith hand-sampling devices, one with a narrow orifice (7.8 cm wide), and one with a larger area orifice (15.2 cm wide). The narrow orifice is of heavier construction, with the advantage of having less of a “parachute” effect when employed during high flows, and is therefore more accurate as it tends not to slide on the bed. The larger area orifice is lighter in construction, and was employed during low-flow times, in order to increase the sampling sensitivity. However, this sampler could not reliably be employed during high-flow events due to its pronounced “parachute” effect. The difference in vertical aperture size in capturing sediment is considered negligible, as no deflection of material off of the orifice was physically detected (e.g. impact vibrations) during sampling.

In order to obtain the most accurate sample of bedload sediment flux possible, it was necessary first to gingerly feel around the bed of the channel (without disturbing any sediment) to find the most topographically flat part available in the channel. The reason being that the streams are quite turbid with silt, and it is

impossible to visually determine if there are any barriers to bedload movement blocking the orifice (i.e. large clasts not in traction). It is also imperative to ensure that the sampling device is not perched on any large clasts preventing the sampler from lying flat on the channel bottom, effectively missing the tracting flux. When such a section of channel bottom is located, the sampler was conscientiously lowered to the channel floor to prevent any disturbance of the bottom sediment when impact occurred. We consciously avoided any tilt of the sampler forward of the angle normal to the bottom of the channel, also known as “scooping”. Scooping can easily occur, and will significantly increase the amount of sediment collected as the flow of the stream becomes disrupted and scouring turbulence is concentrated at the very front of the sampling orifice. For this reason, our data should be considered a conservative “lower limit”.

Because bedload flux can be quite spatially variable, one site of sampling was chosen for each vent, and strictly adhered to throughout the melt season. At both NV and LR, this location was at the transition point between the vent’s outlet and the start of the alluvial reaches. The importance of this location cannot be stressed enough, because this has the distinct advantage of isolating out any fluvial reworking and transport of bedload, thus allowing for the quantification of the true sub-glacial sediment delivery process. Furthermore, both locations were at the middle of the

sediment pathway, so theoretically we were sampling the maximum flux, as tractive and shear stress decrease towards the banks. Samples of bedload were generally taken for three to five minutes of time, with less time allocated for high sediment transport and more time for low sediment transport. This sampling strategy was employed in order to get the most representative values of transport. The samples were then dried and weighed in the field laboratory. The mass of the sediment (in grams) was then divided by the product of the sample time (in seconds) times the width of the sampler orifice (in meters). The latter computation has the benefit of normalizing the two different sampling orifices in terms of a unit width. The resulting value yields a transfer of sediment expressed as flux per unit channel width ($\text{g m}^{-1} \text{s}^{-1}$).

After being dried and weighed, the samples were then sieved through an automated Ro-Tap sieve device for ten minutes to determine the distribution of grain sizes in the sample. The results of the sieving are reported as percent by mass of the total sample mass. Clasts larger than -2.25 phi were not sorted by size and can represent a range of particle sizes, dominated by pebbles. Cobbles are only very rarely present.

Suspended sediment load was obtained through an automated ISCO sampler on an automated sampling schedule. Samples were taken daily at 2-hour intervals,

and reported as concentrations (g/L). These data were then converted to an average concentration value, and multiplied by the average discharge (m^3/s) during the sediment sampling interval, in order to derive a mass per time value suitable for comparison with the bedload data.

Data

Flow data were obtained from a USGS digital nitrogen-bubbler flow recorder for the period of bedload sampling (Figures 1-2a and 1-2b). The discharge data is reported on 10-minute intervals. Peak daily flow for North Vent was $14.7 \text{ m}^3 \text{ s}^{-1}$, occurring on June 28, and $7.4 \text{ m}^3 \text{ s}^{-1}$ at July 15 for Little River vent. Average daily flow is $4.2 \text{ m}^3 \text{ s}^{-1}$ for NV and $2.8 \text{ m}^3 \text{ s}^{-1}$ for LR. The spike in LR discharge on the 10th of July is a result of a culvert removal immediately upstream of the gage and the ensuing draining of the backwater pond, and is not indicative of any physical process at the vent.

Bedload and grain size data for both vents are summarized in Table 1. The average bedload flux (Ave. BLF) through Little River is $1.59 \text{ g m}^{-1} \text{ s}^{-1}$. The average annual bedload flux term for comparison with the average annual suspended load flux (SLF) is:

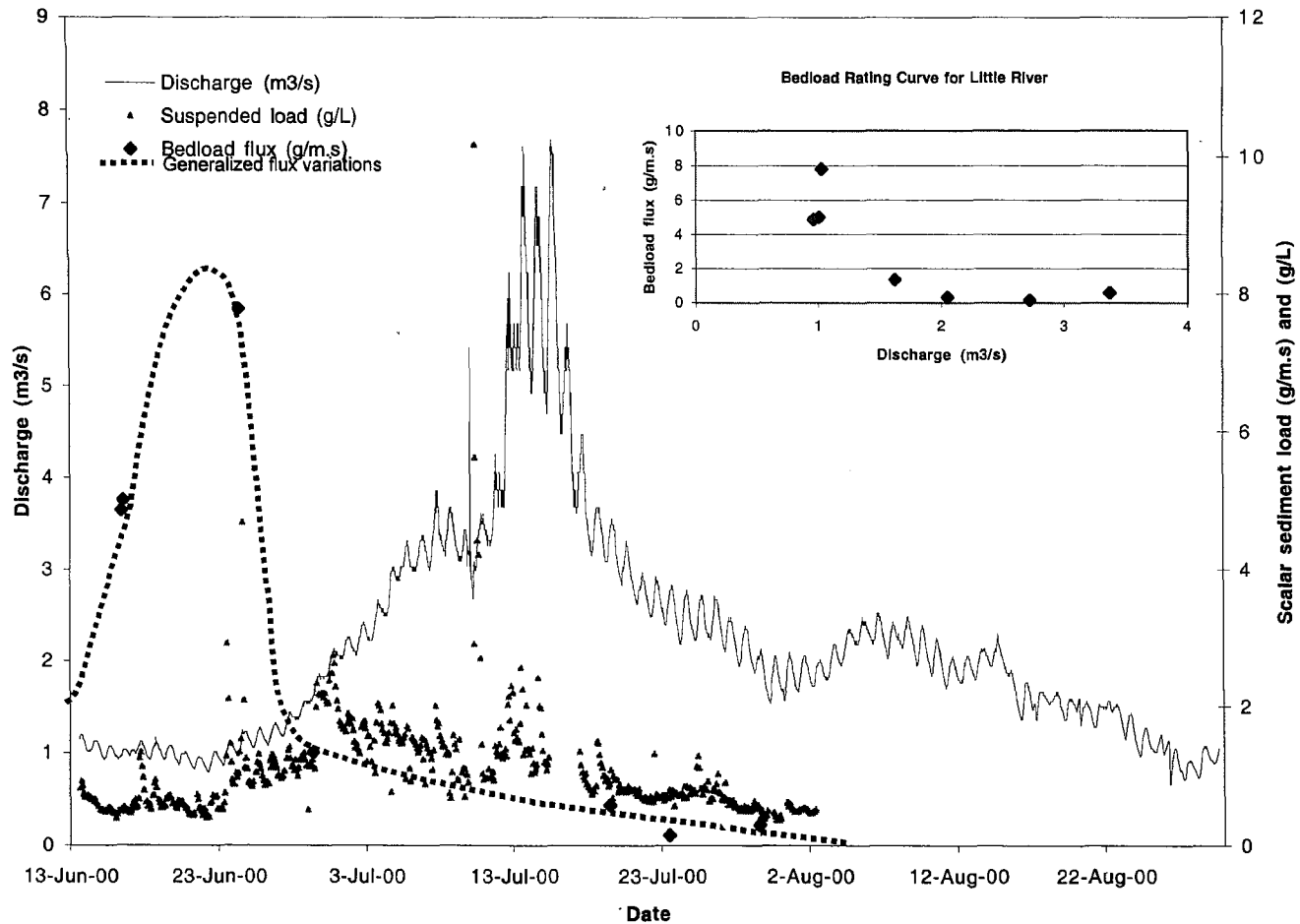


Figure 1-2a. Shows trends in BLF versus SLF in relation to discharge. Dashed line represents generalized flux variation paths, a schematic representation of the system sediment yield behavior. The inset figure plots BLF as a function of discharge.

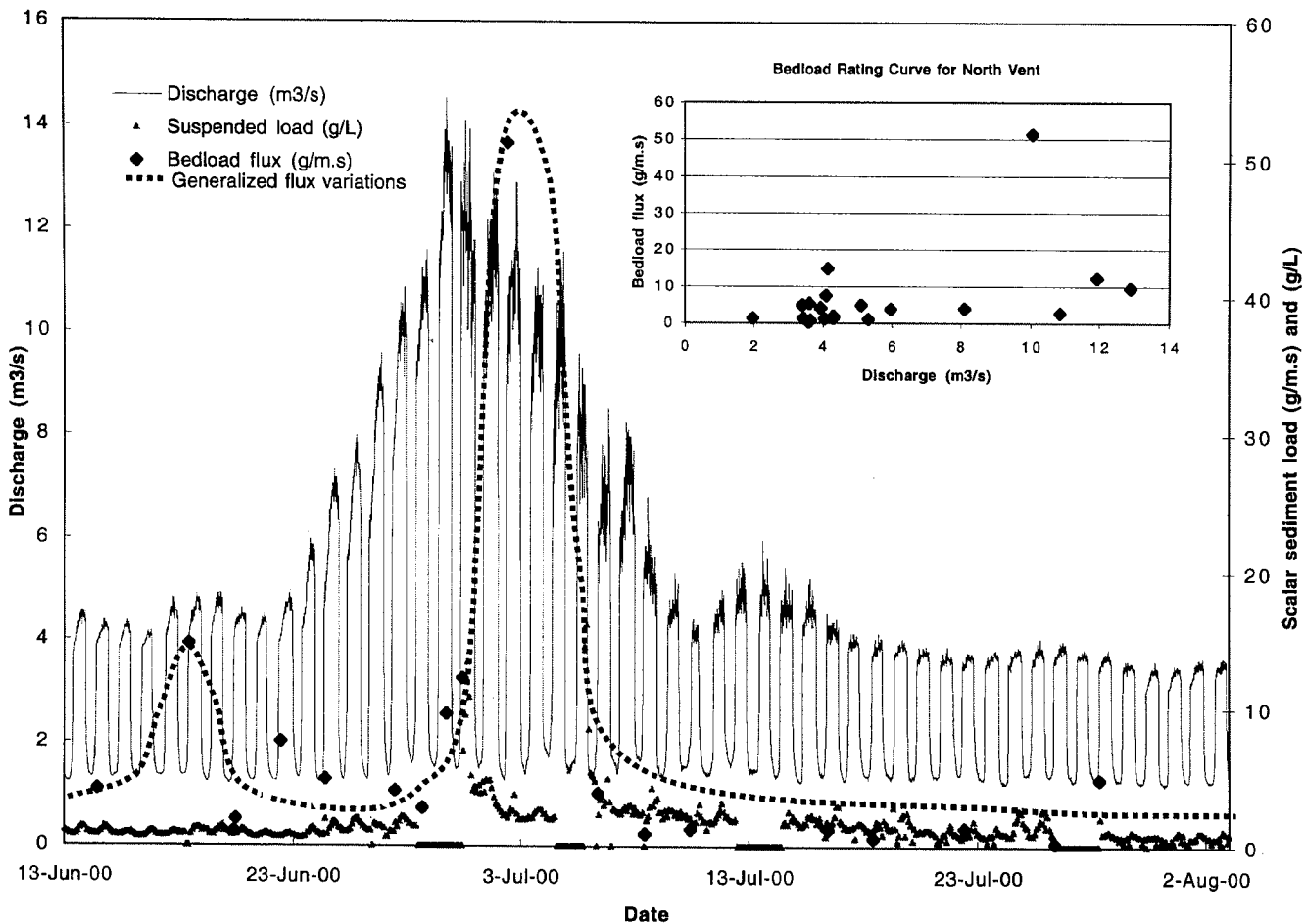


Figure 1-2b. Shows trends in North Vent BLF versus SLF in relation to discharge. Dashed line represents generalized flux variation paths, a representation of the system sediment yield behavior. The inset figure plots BLF as a function of discharge.

Sample Number	Sample date	Sample time	Sample duration (min.)	Sample Location	-2.25 Phi (% by weight)	-1 Phi (% by weight)	0 Phi (% by weight)	1 Phi (% by weight)	2 Phi (% by weight)	3 Phi (% by weight)	Total sed. weight (grams)	FLUX (g/m.s)	% by weight gravel	% by weight sand
3	28-May-00	2:00 PM	3	Little River Vent	0.00%	50.56%	28.33%	15.00%	6.11%	0.00%	0.180	0.01	50.56%	49.44%
6	30-May-00	5:30 PM	3	Little River Vent	0.00%	22.51%	25.65%	37.28%	14.14%	0.42%	0.955	0.07	22.51%	77.49%
7	31-May-00	12:30 PM	6	Little River Vent	0.00%	63.29%	20.55%	12.40%	3.55%	0.21%	2.847	0.10	63.29%	36.71%
8	3-Jun-00	12:30 PM	3	Little River Vent	0.00%	86.38%	10.50%	2.25%	0.87%	0.00%	0.800	0.06	86.38%	13.62%
11	6-Jun-00	2:00 PM	2	Little River Vent	2.56%	26.84%	35.01%	23.54%	11.69%	0.36%	34.677	1.90	29.40%	70.60%
13	10-Jun-00	11:30 AM	3	Little River Vent	15.62%	54.30%	23.47%	5.57%	1.03%	0.00%	1.453	0.11	69.92%	30.08%
16	13-Jun-00	11:30 AM	6	North Vent	94.99%	0.66%	0.71%	1.73%	1.82%	0.09%	111.388	4.07	95.65%	4.35%
17	14-Jun-00	3:30 PM	3	Little River Vent	0.00%	60.68%	27.35%	8.55%	3.42%	0.00%	0.351	0.03	60.68%	39.32%
19	16-Jun-00	12:00 PM	5	Little River Vent	61.84%	24.02%	8.32%	4.22%	1.52%	0.08%	221.754	4.86	85.86%	14.14%
21	16-Jun-00	2:45 PM	5	Little River Vent	68.11%	16.50%	8.23%	4.75%	2.31%	0.09%	228.563	5.01	84.61%	15.39%
23	17-Jun-00	11:15 AM	5	North Vent	88.27%	2.87%	2.40%	3.22%	2.94%	0.30%	670.349	14.70	91.13%	8.87%
25	19-Jun-00	11:00 AM	5	North Vent	30.03%	11.73%	15.35%	22.71%	19.03%	1.16%	46.476	1.02	41.75%	58.25%
26	19-Jun-00	12:35 PM	5	North Vent	30.93%	15.22%	14.70%	19.14%	18.32%	1.70%	86.896	1.91	46.15%	53.85%
27	21-Jun-00	11:45 AM	5	North Vent	62.13%	13.71%	10.00%	8.49%	5.33%	0.35%	343.580	7.53	75.84%	24.16%
33	23-Jun-00	11:00 AM	5	North Vent	43.55%	6.93%	5.23%	7.72%	29.17%	7.40%	218.157	4.78	50.49%	49.51%
35	24-Jun-00	10:45 AM	5	Little River Vent	31.37%	19.22%	12.56%	14.14%	19.28%	3.43%	177.703	7.79	50.58%	49.42%
37	26-Jun-00	12:30 PM	5	North Vent	41.53%	19.62%	13.41%	12.02%	11.41%	2.01%	180.548	3.96	61.14%	38.86%

Table 1-1. Bedload sample masses, fluxes, and grain size distributions.

Sample Number	Sample date	Sample time	Sample duration (min.)	Sample Location	-2.25 Phi (% by weight)	-1 Phi (% by weight)	0 Phi (% by weight)	1 Phi (% by weight)	2 Phi (% by weight)	3 Phi (% by weight)	Total sed. weight (grams)	FLUX (g/m.s)	% by weight gravel	% by weight sand
39	27-Jun-00	5:30 PM	4	North Vent	6.99%	6.37%	5.73%	10.11%	37.71%	33.09%	98.499	2.70	13.36%	86.64%
40	28-Jun-00	5:20 PM	6	North Vent	0.09%	1.28%	4.11%	15.78%	57.66%	21.08%	260.923	9.54	1.37%	98.63%
41	29-Jun-00	10:00 AM	3	Little River Vent	16.03%	27.34%	16.29%	18.40%	20.73%	1.20%	36.377	1.33	43.38%	56.62%
42	29-Jun-00	11:30 AM	3	North Vent	1.56%	2.44%	3.83%	10.84%	63.70%	17.62%	166.437	12.17	4.00%	96.00%
45	1-Jul-00	11:00 AM	5	North Vent	37.05%	2.35%	11.20%	35.14%	12.78%	1.48%	1,167.921	51.22	39.40%	60.60%
50	5-Jul-00	10:50 AM	8	North Vent	39.57%	13.50%	12.80%	19.89%	13.38%	0.86%	138.212	3.79	53.07%	46.93%
52	7-Jul-00	11:30 AM	5	North Vent	4.31%	24.59%	24.05%	28.10%	17.42%	1.53%	19.627	0.86	28.90%	71.10%
55	9-Jul-00	11:00 AM	3	North Vent	27.01%	22.68%	28.45%	15.62%	5.34%	0.90%	16.339	1.19	49.69%	50.31%
57	15-Jul-00	12:00 PM	5	North Vent	6.04%	22.74%	29.02%	26.07%	14.90%	1.24%	27.489	1.21	28.78%	71.22%
60	17-Jul-00	11:30 AM	5	North Vent	2.55%	28.33%	32.35%	26.22%	9.48%	1.07%	13.318	0.58	30.88%	69.12%
61	19-Jul-00	1:40 PM	5	Little River Vent	64.34%	14.82%	7.34%	7.44%	5.48%	0.58%	13.037	0.57	79.16%	20.84%
63	21-Jul-00	11:50 AM	5	North Vent	43.34%	24.23%	15.03%	11.85%	5.12%	0.43%	28.980	1.27	67.57%	32.43%
64	23-Jul-00	2:20 PM	5	Little River Vent	15.63%	41.12%	17.13%	13.09%	11.31%	1.72%	3.147	0.14	56.75%	43.25%
66	25-Jul-00	10:40 AM	5	North Vent	8.69%	8.33%	20.72%	31.53%	28.20%	2.53%	5.015	0.22	17.03%	82.97%
81	27-Jul-00	10:00 AM	5	North Vent	45.06%	24.64%	15.93%	10.54%	3.65%	0.17%	109.445	4.80	69.70%	30.30%
82	29-Jul-00	4:20 PM	5	Little River Vent	37.53%	37.58%	15.62%	5.72%	3.27%	0.28%	6.506	0.29	75.12%	24.88%
84	2-Aug-00	1:00 PM	5	North Vent	24.80%	28.39%	25.62%	16.71%	4.34%	0.14%	121.538	5.33	53.19%	46.81%

Table 1-1. Bedload sample masses, fluxes, and grain size distributions.

$$\begin{aligned} \text{Ave. annual BLF (Metric tons)} = \\ \text{Ave. BLF (g m}^{-1} \text{ s}^{-1}) * 10^{-3} \text{ (kg g}^{-1}) * 31536000 \text{ (s yr}^{-1}) \\ * 0.001 \text{ (metric tons kg}^{-1}) \\ (1) \end{aligned}$$

LR produces an average of 50.2 metric tons of bedload out of the vent per year, per unit channel width. This value is close to the integrated load because the channel width at LR site is approximately 1 meter wide, and the bedload movement is concentrated at the medial portions of the flow.

The average suspended sediment load concentration for LR is 1.066 g L⁻¹.

The following calculation is for the average annual SLF:

$$\begin{aligned} \text{Ave. annual SLF (Metric tons)} = \\ \text{Ave. SLF (g L}^{-1}) * 10^{-3} \text{ (kg g}^{-1}) * 10^3 \text{ (L m}^{-3}) * \text{Ave. Q} \\ \text{(m}^3 \text{ s}^{-1}) * 31536000 \text{ (s yr}^{-1}) * 0.001 \text{ (metric tons kg}^{-1}), \\ (2) \end{aligned}$$

where Q is meltwater discharge. LR discharged an average of 73,286 metric tons of suspended sediment from the vent during the summer of 2000. This reveals that the bedload is 0.07% of the total load, a ratio of 1460:1 (SLF:BLF).

For North Vent, the average bedload flux is 6.64 g m⁻¹ s⁻¹, which results in 209.5 metric tons per year being fluxed out of the vent. In comparison, for the NV, the suspended load computes to be 184,115 metric tons per year. This results in a

ratio of suspended load to bedload of 879:1. Put another way, the bedload is 0.11% of the total load – a rather insignificant portion of the total load. If we assume a constant transport rate across the channel width at the sampling location (~10 m), the integrated bedload flux rises to 1.1% of the total load.

The above calculations are performed assuming a full year of sediment and water discharge activity. In reality, the systems are operate during the months of late May through early October, thus we are overestimating the fluxes. Applying a six month time window to the average fluxes, the sediment yield is halved for the bedload and suspended load. Also, the combined discharge of the two systems accounts for only approximately 25% of the total glacial discharge (J. Denner, pers. comm.). Using the North Vent data as it is considered to be more representative of the system, we see that scaling our average annual flux estimates to represent 100% of the glacial discharge (and, by extension sediment yield), reveals no dramatic increase in the bedload flux (4.4% of total load). However, it should be noted that the two vent systems studied are themselves separate from the other less-accessible vents. Therefore, linearly extrapolating the data to account for these sources should be done with great caution, because the average discharge and sediment flux could be much higher or much lower at those sites.

In direct contrast to the vent data, two tributary streams to the Matanuska River were spot sampled during the early melt season. Hick's Creek, which is downstream of the glacier terminus (Figure 1-1), was sampled on 8-June-00, approximately 550 meters upstream from the junction with the Matanuska River. At this time, snowmelt runoff was very high and the flux of bedload through the sample location was tremendous. The channel bottom was greatly overloose and saltating/tracting clast impacts were distinctly audible. Using the previously described methods and velocity-area discharge calculations, Hick's Creek transported an average of $416.7 \text{ g m}^{-1} \text{ s}^{-1}$ of bedload with an average discharge of $2.15 \text{ m}^3 \text{ s}^{-1}$. The clasts were too big to be sieved, and were generally fist-sized. While the flux magnitude is striking, it should be noted that the previous winter experienced a much larger than normal snowfall, as well as an earlier overall peak discharge, which could make the measurements above average. On the other hand, only half of the Hick's Creek channel could be sampled due to flow intensity, so theoretically, these values should be at least doubled in size. The timing of the sediment delivery from this basin seems to be episodic, yet could be responsible for infrequent evacuation of large slugs of sediment stored on the hillslopes or in channels to the axial trunk Matanuska River, and out of the system.

Grain size data for both of the sub-glacial vent samples are tabulated in Table 1-1. There is much variation in grain size distribution throughout the melt season, and no trend is apparent (Figures 1-3a and 1-3b). For NV, it seems that the grain size increases with discharge, but at LR there are large clasts present at low-flow conditions. On average, the ratio of percent mass of sand to gravel is 62.9:37.1 for NV and 38.7:61.3 for LR. Taken together, these average out to be approximately 50% sand and 50% gravel.

In order to place quantitative constraints as to the potential grain sizes that could be expelled from the vents, preliminary velocity measurements of the vertically directed vent discharge were made. Measurements were taken with a Marsh-McBurney electrical current meter approximately 4 - 5 meters below the water surface for NV and for LR. It is acknowledged that this data collection technique has not been verified for robustness or accuracy, and that turbulent flow, lack of knowledge regarding vent depth and aperture size, and non-verticality of the instrument can all attribute to calculation error. However, initial measurements reveal that at the specified depths vertical uplift speed was $\sim 1.5 \text{ m s}^{-1}$ for NV on 19-June-00, well before peak discharge. Utilizing Stokes law of settling,

$$V^2 = 4/3 \text{ g d } C_d^{-1} ((\rho_s - \rho_f)/\rho_f), \quad (3)$$

Grain size for LR

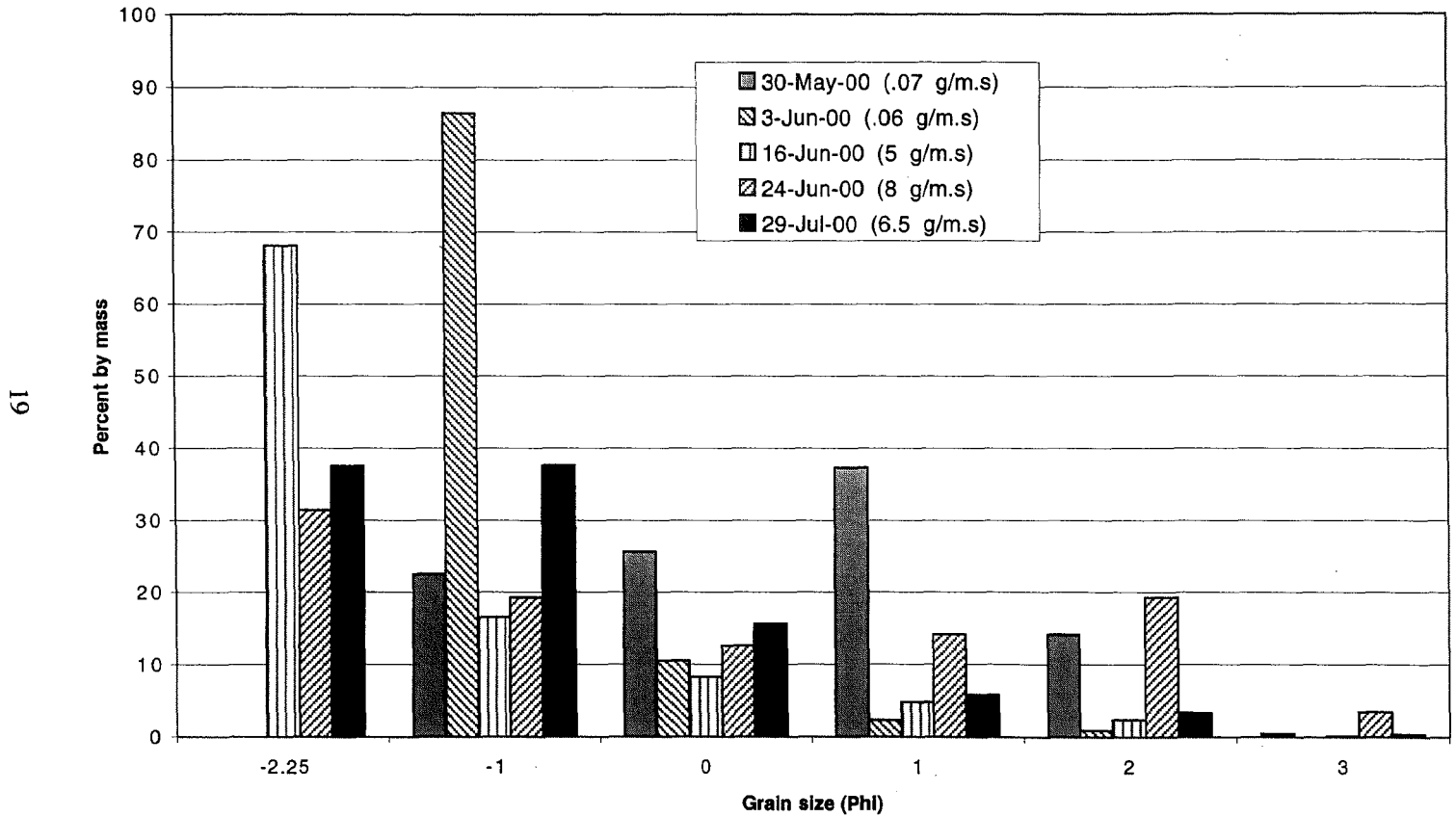


Figure 1-3a. Plot of LR trend in grain size distribution through the meltseason.
Values shown in legend indicates measured flux vaules.

Grain size for NV

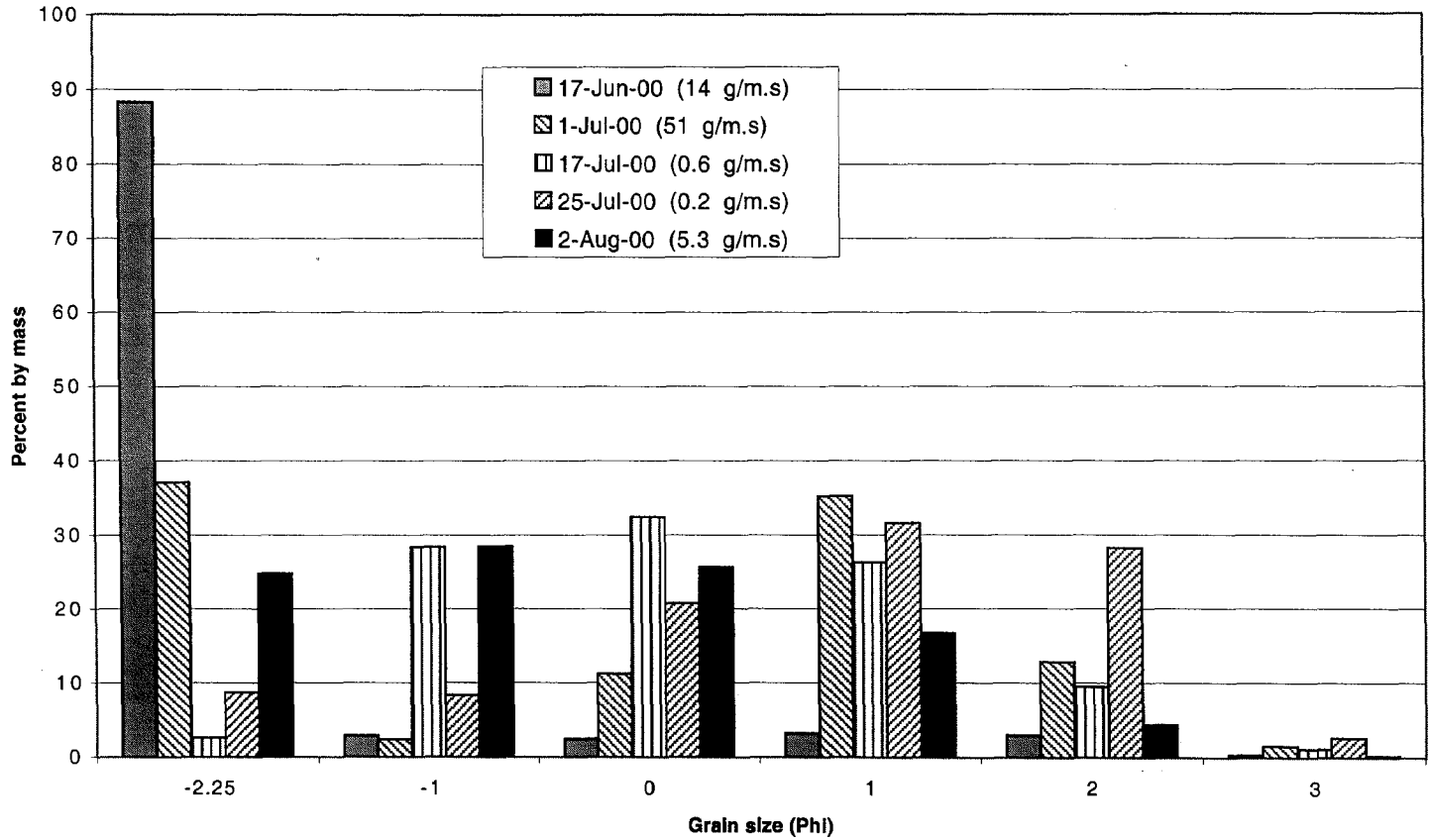


Figure 1-3b. Plot of NV trend in grain size distribution through the meltseason. Values shown in legend indicates measured flux vaules.

Where V is uplift velocity, g is the acceleration of gravity, d is the spherical grain size diameter, C_d is the coefficient of drag (0.6 for greater than sand size particles), and ρ_s and ρ_f as the densities for solid and fluid respectively. A spherical particle with a grain diameter of ~ 6 cm could theoretically be entrained by vent discharge. This uplift velocity is not sufficient to explain the presence of rounded cobbles, much larger than 6 cm, fringing the vent. However, at peak discharge the uplift velocities would be much higher, as inferred from the ~ 1 meter high water fountain that occurs at the vent surface.

Discussion and Implications

Figures 1-2a and 1-2b shows trends in bedload and suspended load in relation to discharge. There are different trends between the two sites in regards to the timing and magnitude of discharge, as well as sediment load delivery. NV had an early season evacuation of bedload, probably related to a reservoir tapping event caused by an expansion of the sub-glacial drainage network. A rise, spike, and exponential decay follow after peak discharge. LR also had a predominantly early season evacuation of sediment, followed by exponential decay in magnitude. High

discharges prohibited samples from being taken at LR vent between 30-June-00 and 18-July-00.

The generalized flux variation paths are also shown on figures 1-2a and 1-2b as the dashed lines, and are to be considered schematic trends. The early season reservoir evacuations of both vents support the theory that linked-cavity type sub-glacial drainage network is important for delivering sediment during the early melt season (Lawson, 1993 p.63). The inset figures show the relationship between discharge and bedload flux. There is poor correlation in the NV data evidenced by the fairly large degree of scatter. There is a striking inverse correlation between discharge and bedload at LR, which strengthens the supposition that these are strongly supply-limited systems. In general, no linear or power-law fit can model the data.

Based on the different timings of discharge, the two vents seem to have different sub-glacial plumbing connections, yet the discharge characteristics for this system are typical for glaciated basins (Figures 1-2a and 1-2b). There is a seasonal rise and fall in discharge during the summer, with the peak discharge usually occurring 1 – 2 weeks after maximum insolation, sometime around mid-July. Superimposed on this curve are smaller wavelength fluctuations in discharge that generally correspond to the diurnal rise and fall in temperature. The discharge

magnitudes begins to decrease near the end of the melt season (early October) as the temperature begins to decrease, and the sub-glacial drainage network begins to “shut down”. Figure 1-2 shows the discharge pattern for the two systems monitored, with the fluxes of bedload superimposed on the plot. The two hydrographs are clearly distinct from one another, with the North Vent experiencing a much larger peak flow on a diurnal, as well as melt season scale.

These sediment yield data are considered to be representative of the sub-glacial sediment delivery process because they follow the discharge and suspended sediment temporal patterns, with a peak flux occurring shortly after the peak discharges (Figure 1-2). This indicates that the sub-glacial drainage network is in fact yielding the load sampled, and we have successfully isolated out any fluvial transportation signals. In addition, the lack of a clear trend in the grain sizes of bedload sampled through the melt season (Figure 1-3) strongly indicates that the sediment is supply-limited by the availability of material trapped in the sub-glacial (basal) ice. This also supports the assumption that the sediment measured is being expelled out of the vent, and not is not a signal of fluvial reworking processes, because in fluvial systems an increase in discharge is correlated with an increase in the size of clasts being transported (competence). The data suggests that for the Matanuska Glacier, no meaningful predictive formulae between BLF and discharge

can be established that would serve to estimate future coarse sediment flux. Alley et al (1997) carefully lay out and quantitatively derive relations for calculating glacially discharged bedload flux, but put forth the caveat that the equations hold only “if the supply of sediment is not limiting” (p. 1018).

Meanwhile, the initial source of the large round to sub-round clasts that are found fringing the vent and immediately downstream in the alluvial channel is still unknown. We put forth the notion that these are not delivered by the vent, but rather are a result of different processes at each location. For LR, which is situated just glacier-side of a moraine, the large clasts are most likely from the breaching of the moraine and the resulting local reworking by fluvial processes, winnowing away finer grained particles. On the other hand, NV is not situated proximal to a moraine, and the angular clasts could be due to the head-ward melting of debris-covered ice as the channel develops, and the subsequent in situ deposition of material. However, the explanation for the source of the well-rounded clasts at NV remains enigmatic.

Since the ratio of the bedload to the suspended load is so small, we can infer several potential scenarios for Matanuska Glacier erosion. First, the glacier mainly creates fine-grained sediment as it abrades its bed, and there is little to no coarse sediment present to be delivered to the sub-glacial drainage network (i.e. abrasion of the bed is the dominant erosional process, and plucking of larger pieces is a minor

process). These processes can be largely influenced by bedrock lithology. Second, there is a much longer storage time for the clasts that are locked in the basal ice relative to the fine grain particles. This statement implies that the sub-glacial drainage characteristics are not of sufficient magnitudes to entrain coarse debris, or stage of development to allow access to sediment reservoirs. This scenario effectively sequesters material for an unknown duration of time. A third scenario is that the major reservoirs of coarse material have long been exhausted by the sub-glacial drainage system, possibly during the large-scale retreat of the Matanuska in the Holocene. This implies that the dominant supply of coarse sediment has passed to the outwash plain $\sim 10^4$ years ago, during a relatively rapid period of time, and we are simply measuring the vestigial remnants of that process.

An alternative to all three of these ideas is that the source of coarse sediment in the valley is not supplied by (steady-state) glacial erosion at all, but rather by erosion and evacuation in the smaller, non-glaciated tributary basins (e.g. Hick's Creek). There are approximately five such basins that drain the north half Matanuska river watershed, and approximately ten that drain the southern portion of the basin. When integrated as a whole, these basins could potentially account for providing a substantial amount of material for valley in-filling. This means that we must re-focus our attention toward this previously overlooked source area as to its role in average

basin-wide denudation. Finally, we do not discount the possibility that there could be a combination of the above mentioned processes in operation at any one time.

The second major implication from the results of our data analysis is that a prescribed ratio of suspended load to bedload cannot be broadly applied to glaciers in general. Matanuska Glacier bedload values account for not more than 1% of the total load, in comparison to other research, wherein bedload ranges anywhere from 30 to 80% of the suspended load (e.g Gustavson and Boothroyd, 1987; Gomez, 1987; Ostrem, 1973; Bogen, 1989). This implies that each glacier is unique in its characteristics of sediment yield, and that a baseline value must be obtained through manual sampling of the individual systems. However, it must be remembered that the Matanuska is potentially a supply limited system, and we may be sampling at a time when the supply is already exhausted. Hence, the predictive quantitative expressions derived by Alley et al (1997), as well as others, should only be employed at transport-limited glaciers.

A primary limitation of the data is that the bedload measurements have only been instituted during one melt season, and only two vents were studied. Although the samples were taken throughout the entire melt season, our interpretations are limited by the relatively low-frequency of sampling, when compared to the suspended load. The possibility remains that the load quantified is could be

atypically lower, or higher, than that of average years. In addition, the two vents being sampled only account for approximately 15% of the total sub-glacial discharge. A complete sampling regimen should be launched to determine if the other vents are contributing more or less quantities of coarse sediment. Also, a more robust method should be developed to quantify peak discharge uplift velocities in the vents in order to better constrain the maximum potential grain size capable of being entrained and delivered out of the vent. However, our data supplies baseline values which the geologic community can utilize to better understand the magnitudes and rates of discharged bedload flux from the glacier, as well as the basin as a whole.

Conclusions

Comparison of the bedload versus the suspended load data reveals that the suspended load comprises > 99% of the total load, and that bedload is a negligible component in any erosion or sediment yield calculations for the Matanuska Glacier. Furthermore, the vents behave as supply limited systems where any sediment fluxing through them is a function of sub-glacial reservoir release. This is significant because this explains why no “power-law” rating curve can be established to relate meltwater discharge to bedload flux. In order to better constrain and verify the 2000 melt season data, more sampling, and/or higher frequency sampling, should be instituted

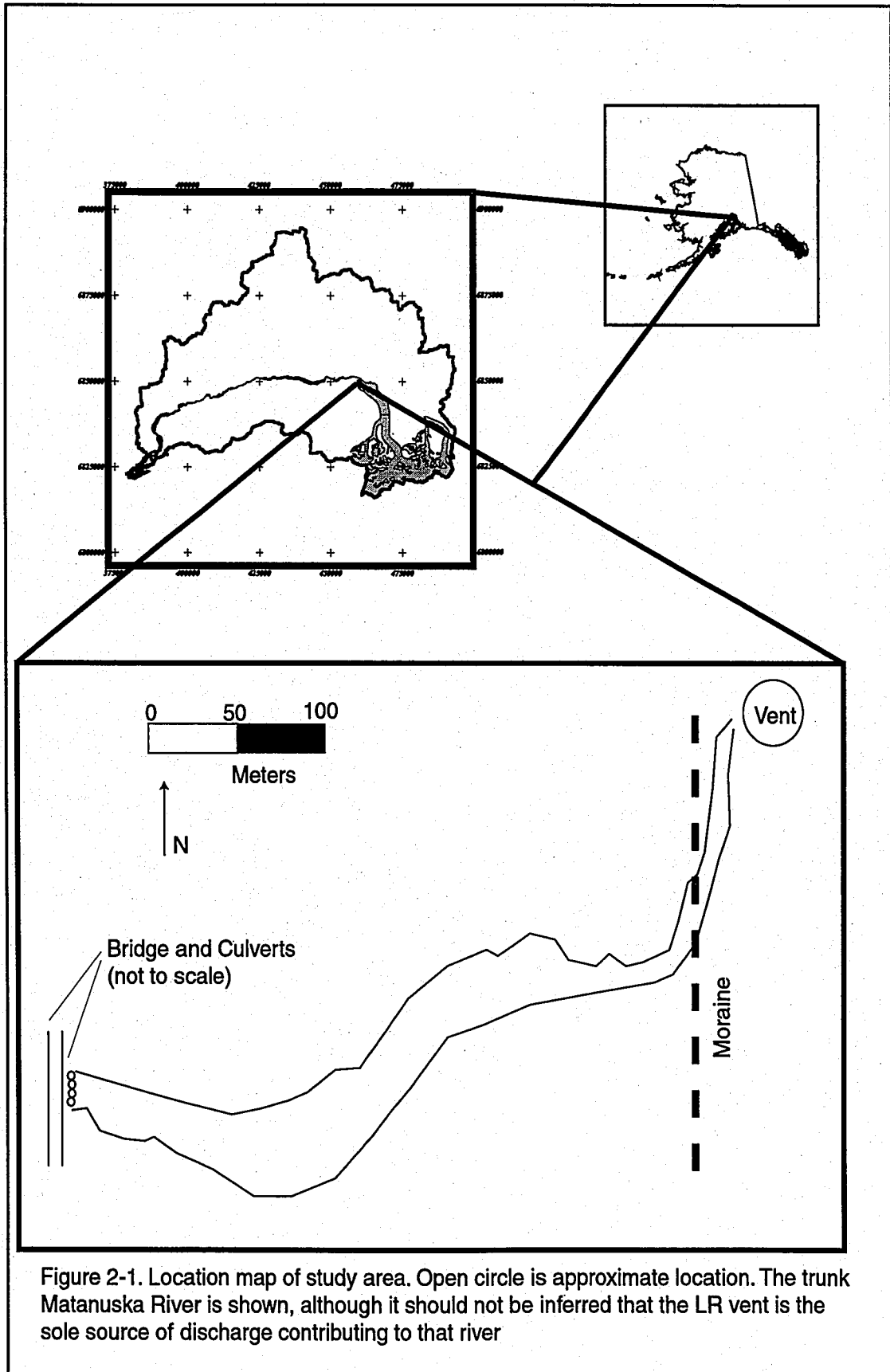
on North Vent as well as other vents. This will provide repeatability and robustness of the data, and it will begin to address the spatial and temporal shortcomings of this research, building a better picture of the decadal-scale variability of sediment yield in this glaciated setting.

Introduction

Discharge, sediment load, and baselevel are perhaps the three most important variables affecting the fluvial system. Significant changes in any, or all, of the variants induce alluvial channels to adjust their form and profile in a predictable manner towards a new equilibrium state. (e. g. Schumm, 1969; Leopold and Bull, 1979; Germanoski and Schumm, 1993; Leopold, Wolman, and Miller, 1964). While flume studies provide an accessible arena in which to investigate the quantitative relationships between fluvial forcings and responses, they cannot adequately capture the true spatial and temporal extent of response in natural channels.

Herein data and observations are presented from a natural, alluvial channel of a particular size and setting such that it can be treated as a large outdoor flume. The setting is a pro-glacial alluvial gravel-bed river in Matanuska, Alaska (Figure 2-1). The outcome of our observations allows us to address such fundamental issues relating to fluvial response time and recovery trends, sediment entrainment and mobility concepts, local base-level fluctuations, and vertical versus lateral incision processes.

Initially, our motivation was to examine the system in order to quantify and describe how such a system responds to variations in discharge and sediment load over a glacial melt-season. Since we did not have first-hand experience with this



field area and its associated surface process behaviors, we were not certain whether the fluvial system would be static or dynamic. Oral communication with workers in the area delivered conflicting views as to the activity of the system. On one hand, there were reports that the same gravel bars had been in the same location for years with no noticeable change in geometry. In contrast, there were reports that one could audibly hear the cobbles of the channel bed being rolled and bumped along the bottom. These two statements are virtually mutually exclusive. In other words, there cannot be a high degree of sediment movement in conjunction with a static channel form.

We began our study just upstream of bridge and culvert arrangement, so that we were not hampered by any anthropogenic factors (Figure 2-1). These culverts reached maximum capacity before peak discharge occurred, instigating a backwater pool and subsequent local aggradation. In order to avoid catastrophic failure, the culverts were pulled out on 10-July-00 and replaced with a structure of much larger capacity. We focussed our attention on the sudden drop in local baselevel, the resultant draining of the stored sediment and water, and documented the pre-, syn-, and post-forcing dynamics of this braided alluvial channel. It will be demonstrated that this stream in particular responds in a very non-linear fashion, and that the temporal nature of the response magnitude is exponential decay with a complex

response of alternating sediment storage and evacuation. Furthermore, we will examine the effects that baselevel rise and fall had on the upstream portions of channel, and how far the perturbation was propagated through the system.

Physical Setting

The specific location of our study area is at the terminus of the Matanuska glacier, approximately 100 miles northeast of Anchorage, Alaska, just off of the Glen Highway (Figure 2-1). The particular reach examined, dubbed Little River (LR), is approximately 350 meters in valley length and has its headwaters in a subglacial “vent”, where subglacial melt water is discharged. The vent has a lacustrine-type morphology, with the subglacial discharge appearing as a small fountain in the middle of the body of water when sub-glacial hydrostatic pressure builds up. The vent for Little River is surrounded by hillslopes of vegetation-free, debris-covered ice (Figure 2-2). The ice melts as the summer progresses, instigating many small-scale mudflows. These mudflows are a dominant process in delivering coarse and fine sediment to LR’s headwaters, and are referred to as “inwash”. Directly downstream of the vent, the stream breaches a moraine-ridge approximately 10 meters in height, and 5 meter in width (Figure 2-2). The valley bottom is virtually non-existent in this reach until the moraine is passed, where the valley bottom abruptly widens and a large numbers of boulders are found in the channel and “floodplain”. There are no tributary inputs along the reach studied, therefore discharge is considered constant downstream (e.g. Chew and Ashmore, 2001).

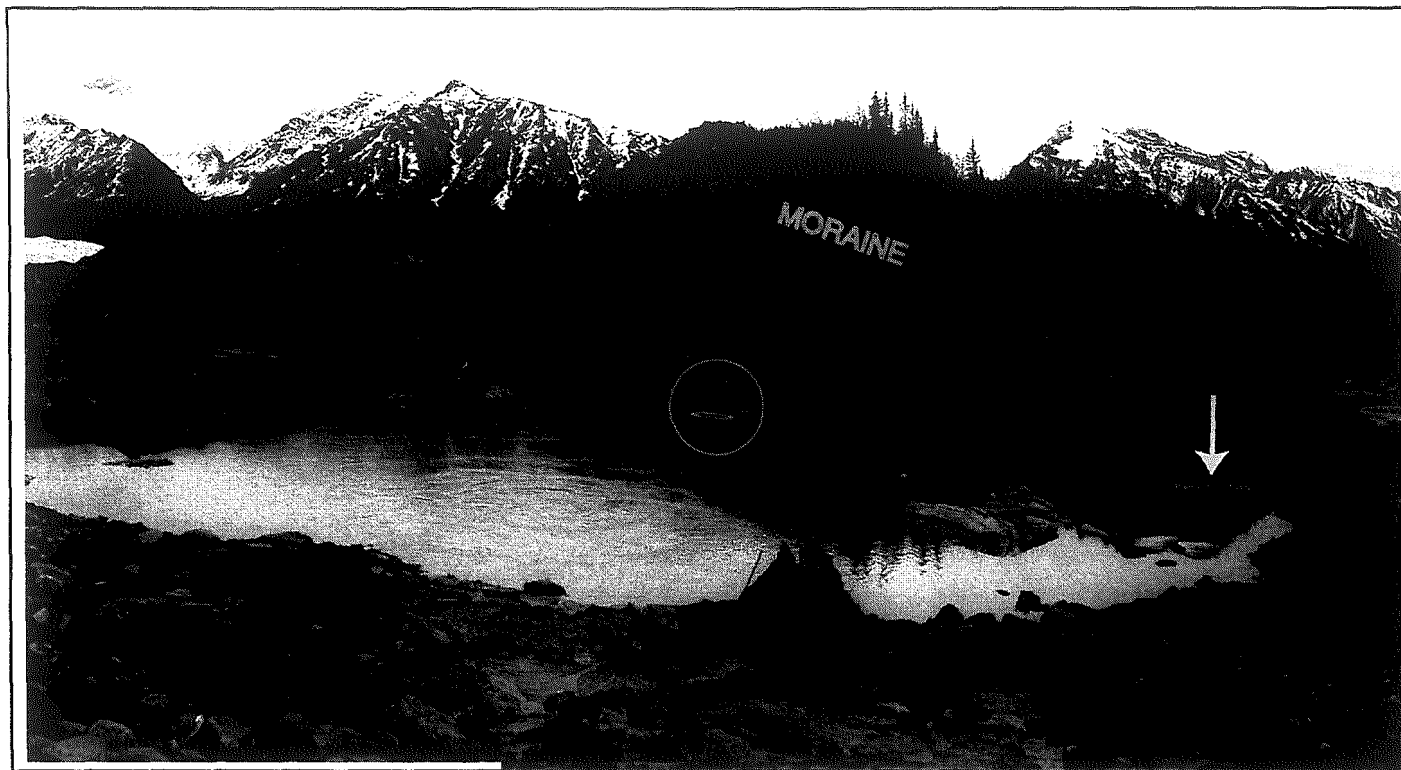


Figure 2-2. Little River Vent. Vent to channel transition is at the right of the page. Note person for scale, instability of hillslopes, and incision of moraine. Vent bedload sample location is indicated by white arrow.



Figure 2-2. Little River Vent. Vent to channel transition is at the right of the page. Note person for scale, instability of hillslopes, and incision of moraine. Vent bedload sample location is indicated by white arrow.

Baseflow and/or losing reaches are considered negligible. The system can receive additional discharge in the form of precipitation and surface runoff. During the 2000 field season, there were no significant storm events that contributed to the overall discharge of the LR.

Channel characteristics

Little River is representative of typical braided rivers: a wide and shallow channel profile, an overall large median grain size, downstream fining, steep energy slopes, and multiple channels (anabranches) separated by sub-areally exposed bars. These bars may or may not be vegetated, and vary in size while retaining characteristic parabolic lobate shapes with “tails” pointing upstream. The bars usually have high percentage of fines in the interstices of the clasts. This is due to the large amount of suspended sediment in the water, which tends to drape over the bars as small scale bar flooding occurs. The vegetation is composed primarily of large shrubs, which can reach approximately 2-3 meters in height (Figure 2-3).

Discharge

The discharge characteristics for these systems are typical for glaciated basins (Figure 2-4). There is a large wavelength rise and fall in discharge during the melt season, with the peak discharge usually occurring 1 – 2 weeks after maximum insolation, sometime around mid-July. Superimposed on this curve are smaller wavelength diurnal fluctuations that generally correspond to the rise and fall in temperature. The discharge pattern begins to behave erratically near the end of the

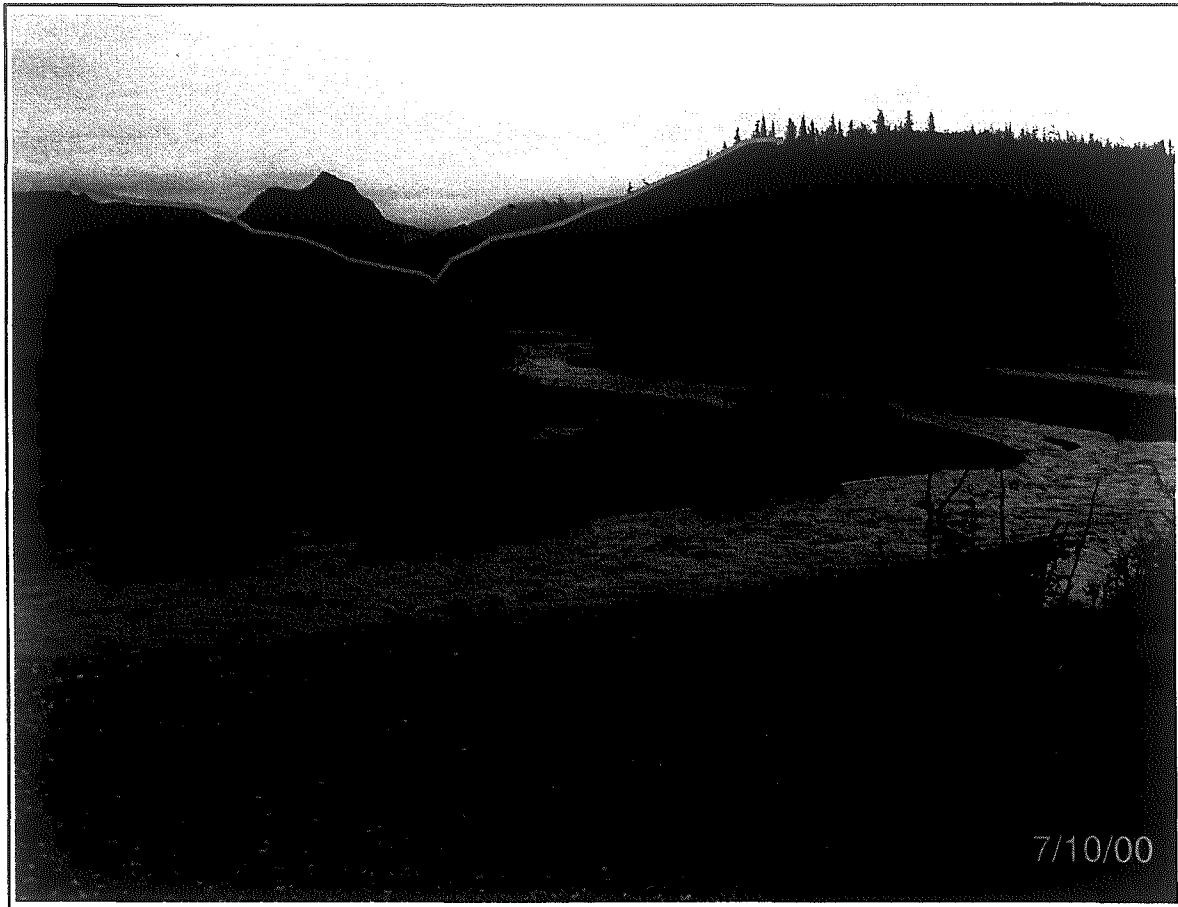


Figure 2-3. Upstream view of LR showing vegetated and bare bars. Line depicts approximate location of moraine that is breached. Location of picture is approximately 5 m north of (0,0) on Figure 5.

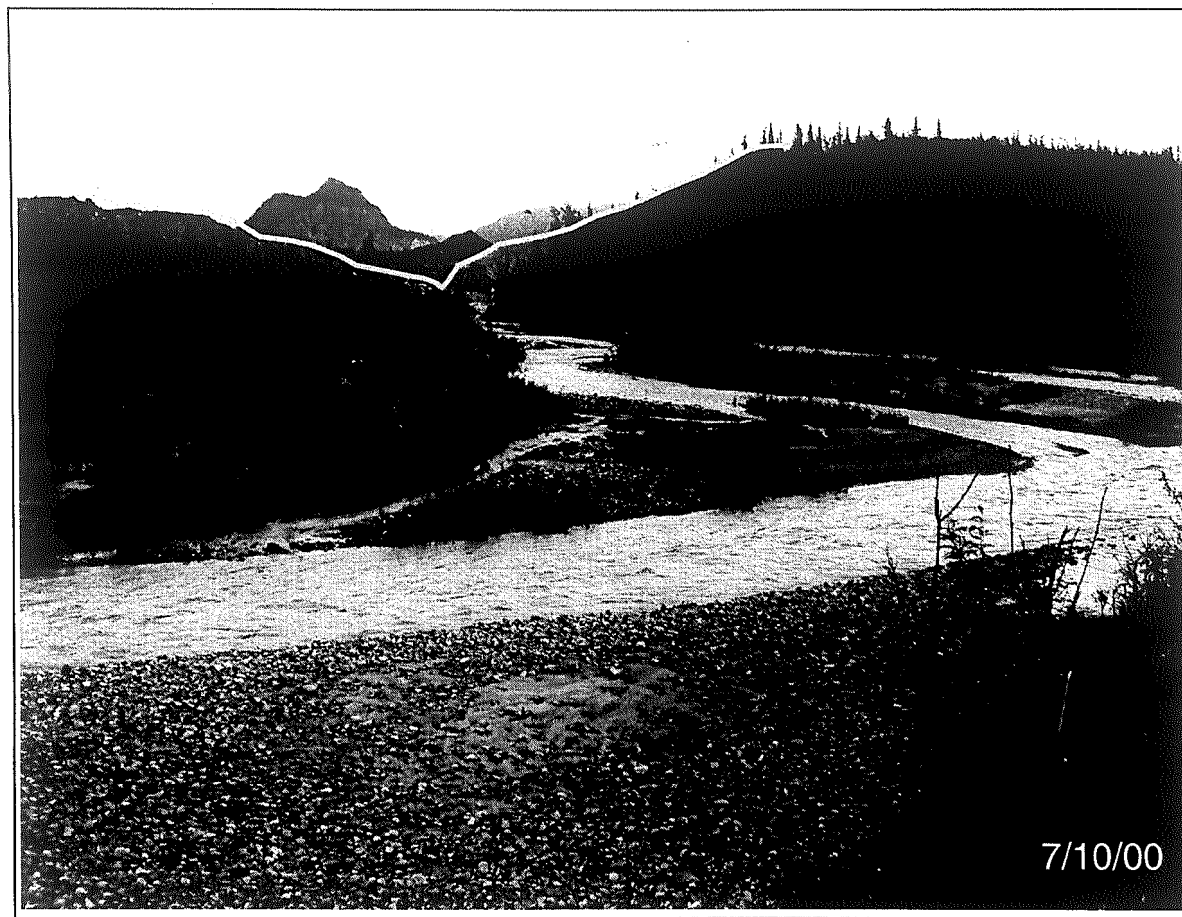


Figure 2-3. Upstream view of LR showing vegetated and bare bars. Line depicts approximate location of moraine that is breached. Location of picture is approximately 5 m north of (0,0) on Figure 5.

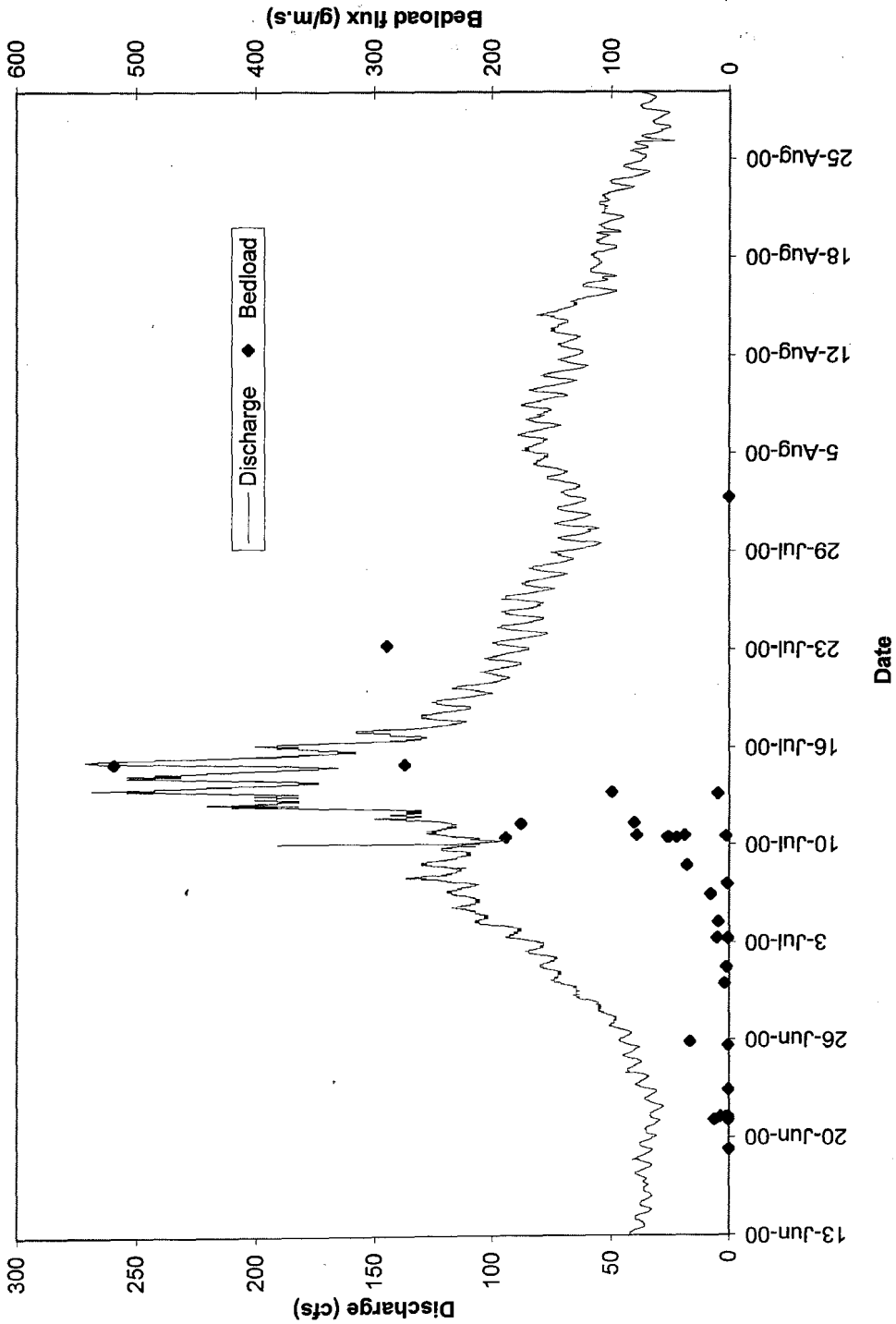


Figure 2-4. Little River hydrograph with bedload flux data

melt season (mid- late-August) as the temperature begins to decrease, and the subglacial drainage network begins to “shut down” (Lawson, 1993).

Culvert

Little River braids naturally downstream of the moraine, with the individual channels converging shortly up stream of a wooden bridge (Figures 5a and 5b). In order to ensure stability of the bridge, four corrugated steel culverts collect and route the flow under the bridge. These four culverts have a combined capacity of approximately 120 cfs, and began to approach maximum capacity in early July. This initiated a backwater ponding effect, with a slack pool forming where the flow velocity subsides. Since the water is highly laden with glacial silt, a “clay ring” was deposited on the edges of the water surface against the bank, marking the elevation and slope of the water surface in the backwater pond. In effect, this system can be conceptualized as a dam and reservoir system, with a controlled release (the maximum capacity of the culverts). This scenario also serves to simulate a local base-level rise to the fluvial system

As the culverts were at maximum capacity before the seasonal peak flow was reached, the property owners decided to replace them with a single, much larger capacity half-pipe. This removal operation took place between the late night hours of July 9th and the early morning hours of July 10th. Simulating a local and sudden

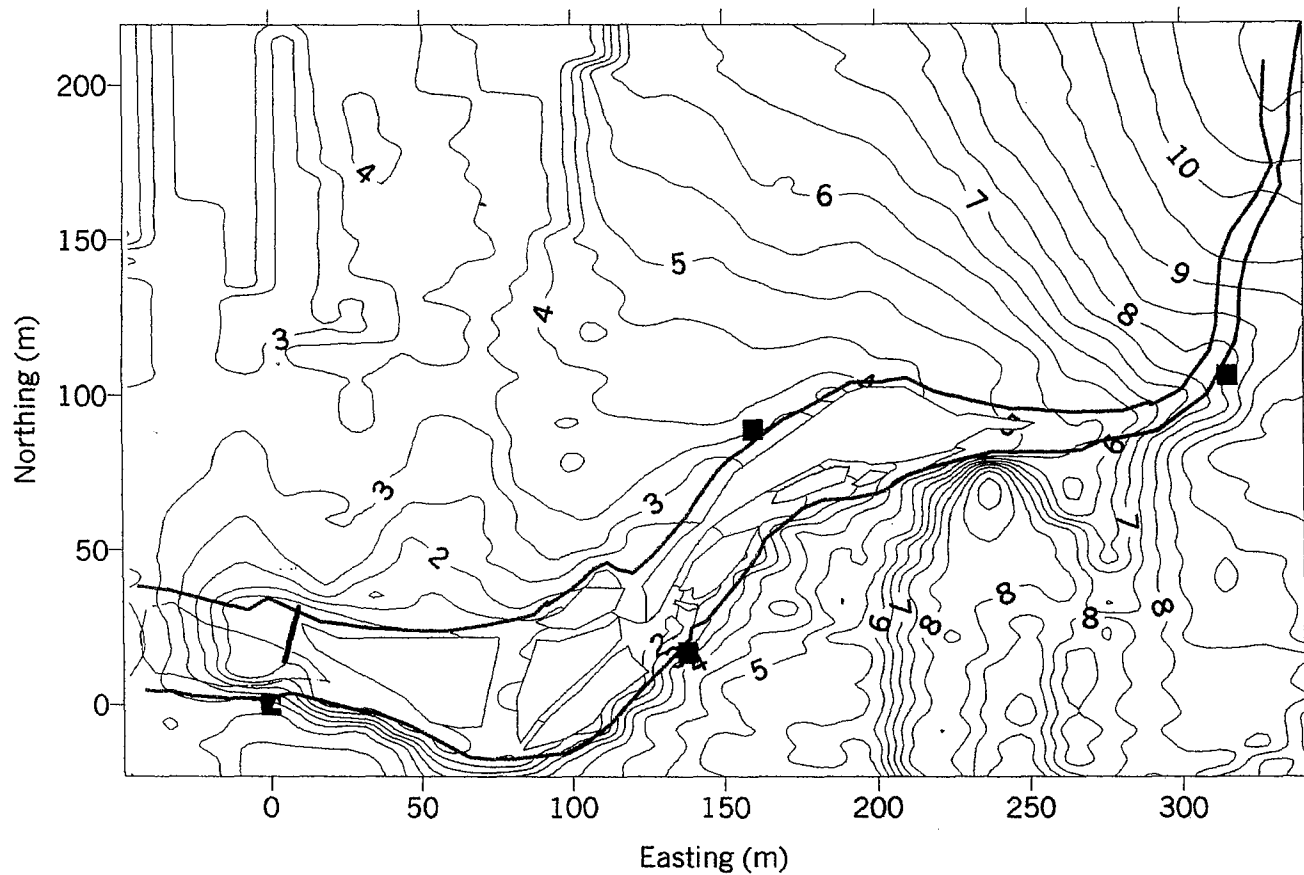


Figure 2-5a. Early season channel morphology. Cross section line shown in blue. Location of culverts are approximately (-45, 35).

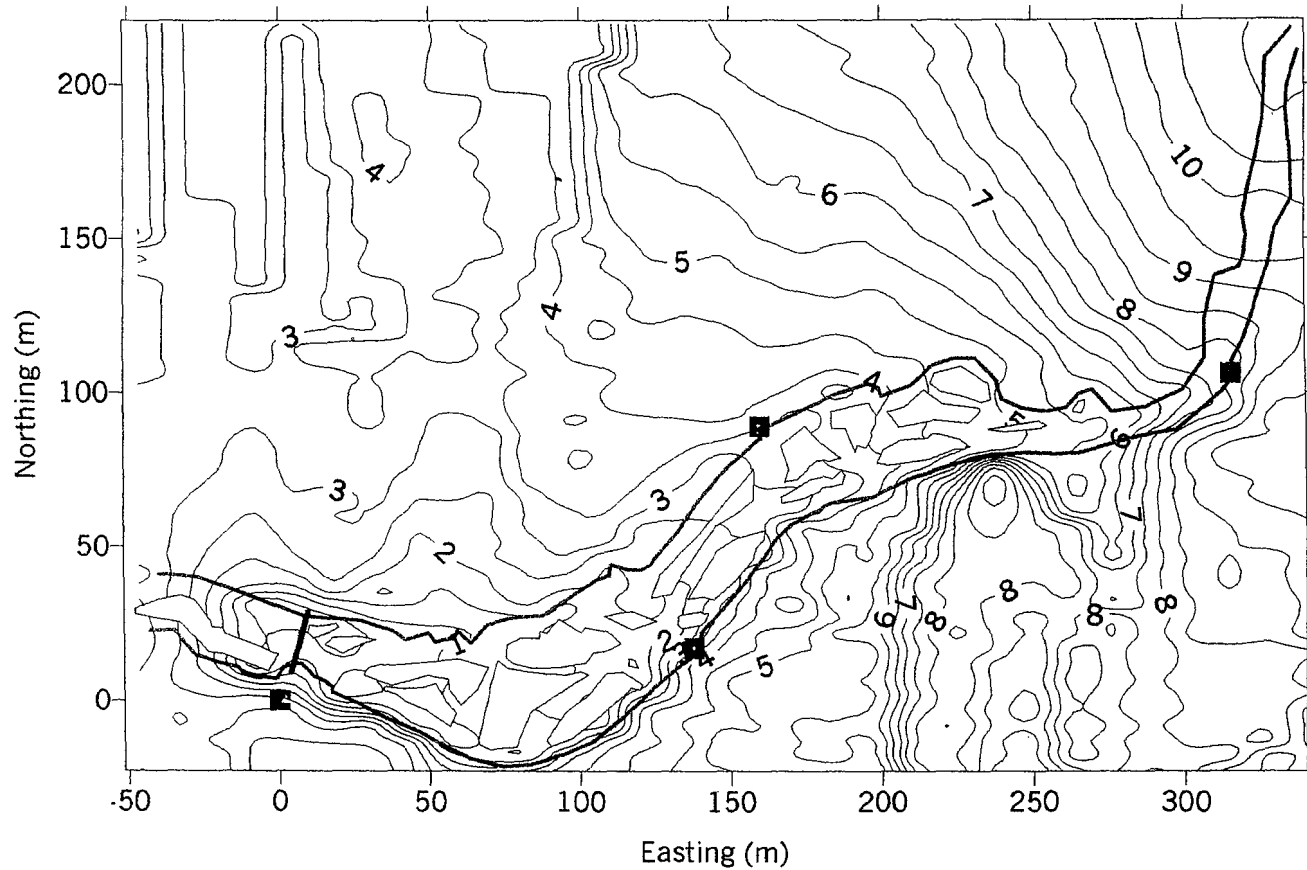


Figure 2-5b. Late season channel morphology. Note the dissection of pre-existing bars as the water surface rises.

base-level fall, this action had profound and immediate impacts on the fluvial system, which is described below.

Methods

Bedload

Bedload data was collected using two Helley-Smith hand-sampling devices, one with a narrow orifice (7.8 cm wide), and one with a larger area orifice (15.2 cm wide). The narrow orifice was of heavier construction, with the advantage of having less of “parachute” effect when employed in high flows. The larger area orifice was lighter in construction, and was employed during low-flow times, in order to increase the sampling sensitivity. However, this sampler could not reliably be employed during high-flow events due to its pronounced “parachute” effect. The difference in vertical aperture size in capturing sediment is considered negligible.

In order to get the most accurate sample of bedload sediment flux possible, it was necessary to carefully feel around the bed of the channel (without disturbing any sediment) to find the most topographically flat part available in the channel. This is because the streams are very turbid, and it is impossible to visually determine if there are any barriers to bedload movement blocking the orifice (i.e. large clasts not in traction), as well as to ensure that the sampling device is not perched on any large

clasts. When such a section of channel bottom was located, the sampler was carefully lowered to the channel floor to prevent any disturbance of the bottom sediment when impact occurred. A concerted effort was made to avoid any tilt of the sampler forward to the angle normal to the bottom of the channel, also known as “scooping”. Scooping can easily occur, and will significantly increase the values taken as the flow of the stream becomes disrupted and turbulence is concentrated at the very front of the sampling orifice. For this reason, our data can be considered to be a conservative “lower limit”.

Because bedload movement in alluvial channels can be quite spatially variable, two sites of sampling were chosen, and strictly adhered to throughout the melt season. The first location was at the transition point between vent and channel (Figure 2-2). This site (LR Vent) was chosen so that any sediment that was being delivered to the stream via subglacial processes could be quantified. This also has the advantage of setting a beginning value of bedload flux at the headwaters of the stream. The second site was located approximately 300 meters downstream from the vent (Figure 2-5). A cross-section line was established at this point, so that the same location could repetitively be sampled throughout the melt season. This site (LR X-sec) was chosen because it was the only downstream reach where the braided

channels converged into one main channel, thus allowing for an integrated downstream measurement of bedload flux.

Samples of bedload were generally taken for three to five minutes of time, with less time allocated for high sediment fluxes, and more time for low sediment fluxes. This was done in order to get the most representative values of load. The samples were then dried and weighed in the field laboratory. The mass of the sediment (in grams) was then divided by the product of the sample time (in seconds) times the width of the sampler orifice (in meters). The resulting value gives a flux of sediment expressed as mass per unit time per unit width of channel. This also has the benefit of normalizing the two different sampling orifices in terms of a unit width. After being dried and weighed, the samples were then sieved through an automated Ro-Tap sieve device for ten minutes to determine the distribution of grain sizes in the sample. The results of the sieving are reported as per cent by mass of the total sample mass. Clasts larger than -2.25 phi were not sorted by size and can represent a large range of particle sizes. Any data reported as 100% -2.25 phi by mass are samples that were not sufficiently dry to be sieved, and in actuality contain smaller grain sizes.

Survey

In order to document the changes in the fluvial geomorphology during the melt season, it was necessary to create a topographic basemap of the reach being studied, which includes the braided channel patterns as well as the valley floor topography. This was accomplished using a TDS-211 digital total station.

A total of five complete topographic maps were created during the melt season. Of the five, only three are useable, as the first survey had uncorrectable errors arising from the transition from base stations, and one survey was incomplete. The topographic surveys were organized such that there was one shot in the beginning of the melt season (late May), one in the middle (late June) and one near the end of the season (late July). In addition, data on observed local changes in channel morphology and energy surface slope were documented by numerous larger scale surveys. For comparison sake, the only surveys presented are pre- and post-baselevel fall.

Braid bars

To facilitate the determination of the mobility of coarse sediment in the system, three braid bars were selected, and their areal boundaries were marked by means of pounding in metal stakes via sledgehammer at the beginning of the melt season. These bars are aligned along the major axis of flow, with the most upstream

bar having the highest d_{50} . The grain size was determined by a 10 cm spaced pebble count along the long axis of the bars, using digital calipers and a blind, random grab technique to avoid optical biasing. By surveying in the bar outlines with the total station, their position in space can be accurately determined. These bars were tracked throughout the flow season to determine the magnitude of movement, if any.

Data

Survey

The early summer (June 2, 2000) and the late season (July 28, 2000) surveys are plotted in figures 2-5a and 2-5b. The figure shows that the main channel banks (red lines) are stable throughout the melt season. There is very little overall change in channel width, as measured between the banks. Any observed increase is attributable to an increase in the water surface elevation from increased discharge. Figure 2-5b shows an increase in the braiding intensity compared to 2-5a. However, this again is due to the rise in water surface elevations, causing the bars to become flooded down their axial lows, and hence become dissected by flow. This apparent equilibrium is supported by the fact that the gravel bars do not change their overall position, and are most likely stalled (Germanoski and Schumm, 1993).

Long Profiles

Channel longitudinal profiles from the beginning and the end of the flow season are shown in Figure 2-6a. South bank profiles are used because individual channel water surface elevations can vary naturally (Germanoski and Schumm, 1993), and also because the southern bank is where the monitored geomorphic work occurred. The headwaters of LR are flat in the long profile as the channel passes through the moraine (between 500 and 600 meters distance in Figure 2-6a). The two profiles show typical concave up shapes, and steep overall gradients. There is no significant profile change incurred by a full summer melt season, indicating a system that is more or less at grade to the given discharge. The localized convexities in the profiles indicate slugs of sediment being stored in the channel. That they do not migrate downstream during the meltseason supports the inference that they are indeed stalled bars. This implies that the channel has graded to much larger peak flows than currently measured, and is not significantly attempting to establish a new equilibrium profile. The profiles intersect at approximately 100 meters distance (Figure 2-6a), and here the late season profile shows an abrupt increase in slope, most likely due to the localized baselevel fall. Figure 2-6b is a close-up of the surveys to explore this idea in more detail.

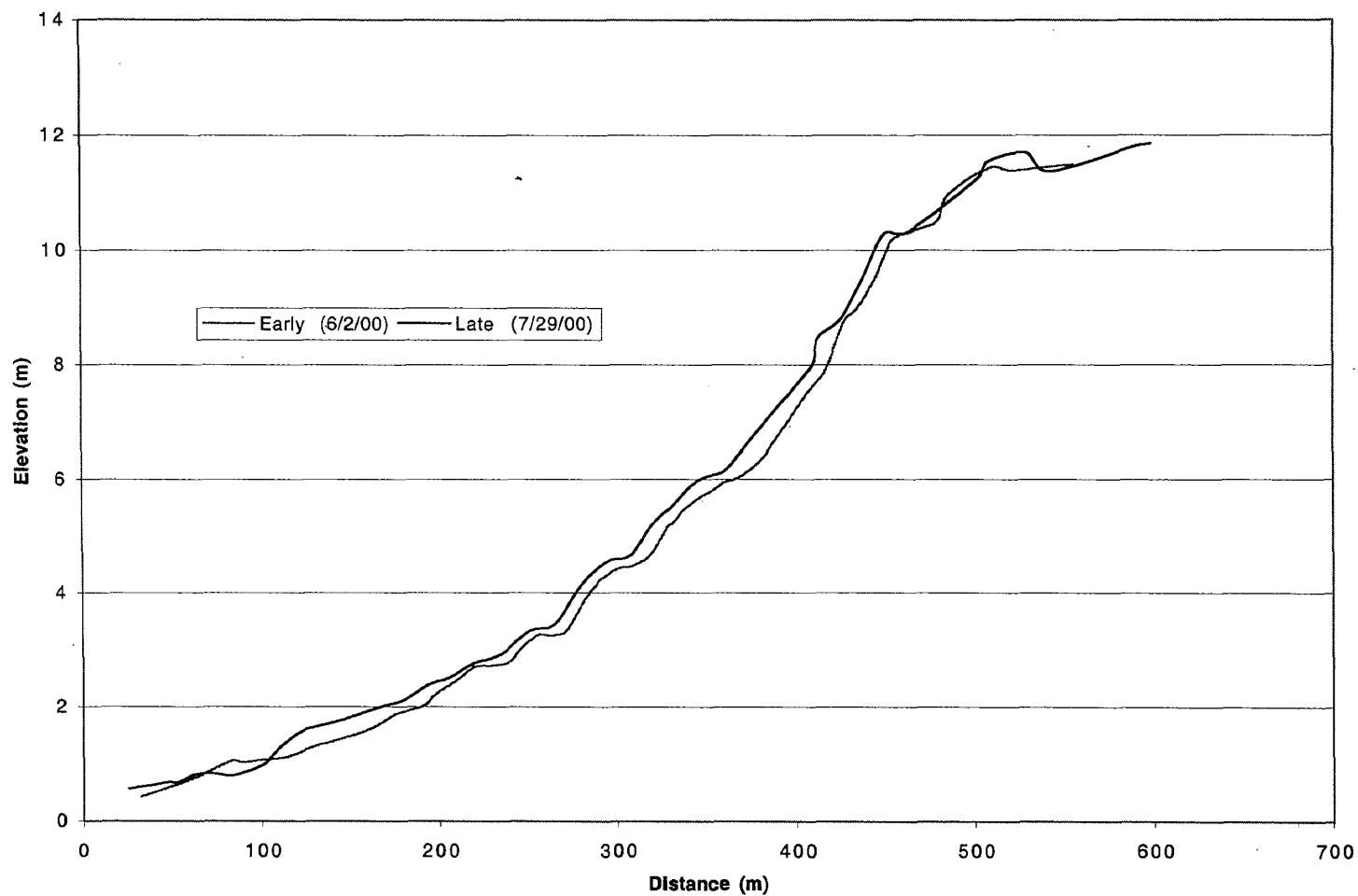


Figure 2-6a. Little River south bank long-profile comparison.

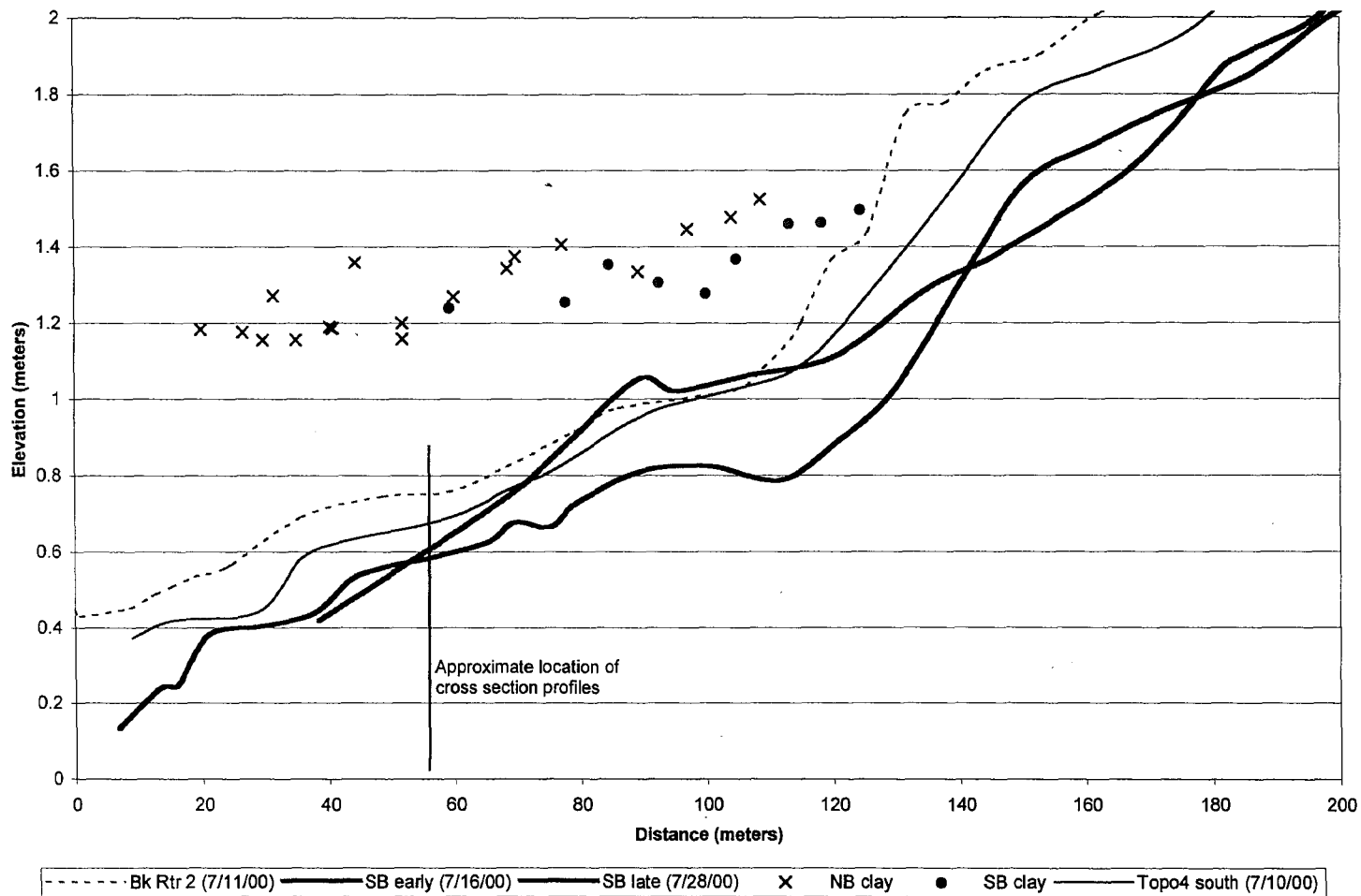


Figure 2-6b. Long profiles and clay ring elevations from backwater area.

Figure 2-6b shows the longitudinal profiles of the clay ring elevations, from both the north bank and south bank of the channel. Also included are the long profiles of the water surface elevation (energy slope) from June 2, July 10, July 16, and July 28 to show the pre-culvert removal slope, and the evolution of the profile after culvert replacement. For the sake of reference and context, the position of the cross sectional profiles relative to the long profiles is placed on Figure 2-6b.

Channel Cross Sections

Four channel cross section surveys were performed during the flow season (Figure 2-7); one in the early flow season, one closely following culvert removal, one about a week after removal, and one near the end of the flow season. Figure 2-7 shows the downstream view, with flow being “into the page”. The cross section was constructed approximately fifty meters upstream of the culvert (Figure 2-5). The “south” channel received a small amount of flow early in the season, but emptied and never re-filled after July 10.

Flow

Flow data were obtained from USGS digital flow recorder for the period of 16-June to 28-Aug (Figure 2-4). Prior to this time, discharge was measured via velocity-area relationship. The hydrograph data is reported on 10-minute intervals.

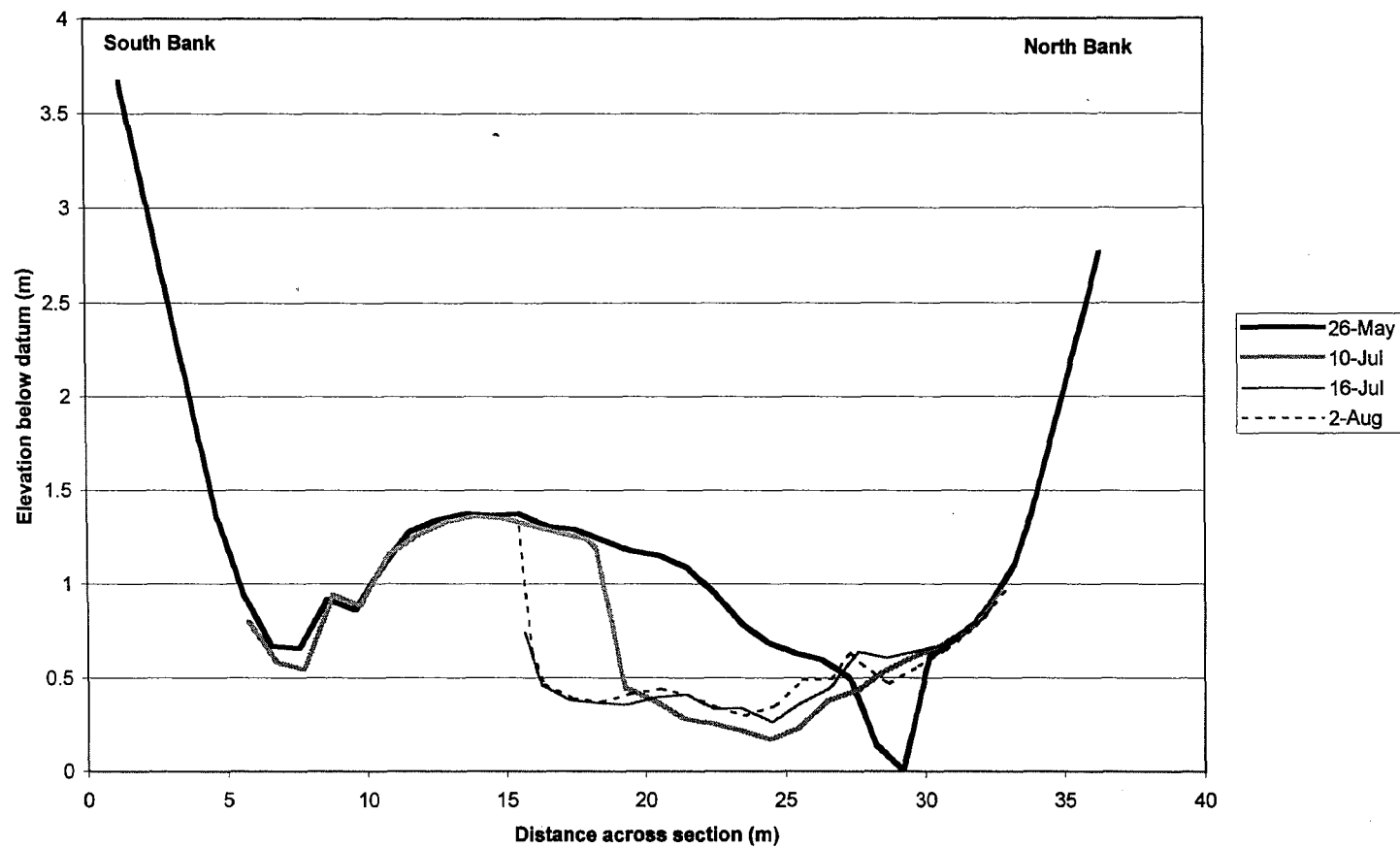


Figure 2-7. Little River cross section profiles. View is in the downstream direction (see figure 5 for location).

Peak flow was 260 cfs, occurring on July 15. Flow goes to near 0 when the winter freeze halts discharge. Average flow is 100 cfs, and median flow for the summer of 2000 is 70 cfs. The spike in discharge on the 10th of July is a result of the culvert removal and the ensuing draining of the backwater pond, and not indicative of any physical process.

Bedload

Bedload data are summarized in Table 2-1. The average transport rate of bedload through Little River prior to culvert removal is $1.51 \text{ g m}^{-1} \text{ s}^{-1}$. This value has an implied per unit channel width term, as it is a part of the flux measurement dimensions. However, this is justified as the channel being studied is not very wide at sample point (Figure 2-7), and that bedload movement decreases towards the channel edges as the flow velocity, and therefore shear stress, decreases. Maximum flux measured is $823.43 \text{ g m}^{-1} \text{ s}^{-1}$, recorded on the 10th of July. Average bedload flux following culvert removal is $145.28 \text{ g m}^{-1} \text{ s}^{-1}$. By default, minimum bedload is 0. There is no correlation between the movement of bedload and the magnitude of discharge (Figure 2-8).

Note: Site 1 = Little River Cross-section, Site 2 = Vent

Sample Number	Sample date	Sample time	Sample duration (min.)	Sample Location	-2.25 Phi (% by mass)	-1 Phi (% by mass)	0 Phi (% by mass)	1 Phi (% by mass)	2 Phi (% by mass)	3 Phi (% by mass)	Total sed. mass (grams)	FLUX (g/m.s)	% by mass gravel	% by mass sand
1	28-May-00	11:00 AM	3	1	0.00%	13.96%	21.49%	31.48%	30.31%	2.77%	2.959	0.22	13.96%	88.04%
2	28-May-00	1:00 PM	3	1	0.00%	77.95%	18.02%	4.21%	1.85%	0.18%	2.852	0.21	77.95%	22.05%
3	28-May-00	2:00 PM	3	2	0.00%	50.58%	28.33%	15.00%	6.11%	0.00%	0.180	0.01	50.58%	49.44%
4	29-May-00	3:00 PM	3	1	0.00%	20.18%	0.00%	15.78%	57.02%	7.02%	0.228	0.02	20.18%	79.82%
5	29-May-00	8:00 PM	3	1	0.00%	58.14%	2.82%	7.04%	31.19%	3.02%	0.497	0.04	58.14%	43.86%
6	30-May-00	5:30 PM	3	2	0.00%	22.51%	25.65%	37.28%	14.14%	0.42%	0.955	0.07	22.51%	77.49%
7	31-May-00	12:30 PM	6	2	0.00%	63.29%	20.55%	12.40%	3.55%	0.21%	2.847	0.10	63.29%	36.71%
8	3-Jun-00	12:30 PM	3	2	0.00%	88.38%	10.50%	2.25%	0.87%	0.00%	0.800	0.06	88.38%	13.62%
9	5-Jun-00	10:00 AM	3	1	0.00%	8.83%	4.03%	12.99%	60.39%	13.77%	0.770	0.06	8.83%	91.17%
11	6-Jun-00	2:00 PM	2	2	2.56%	26.84%	35.01%	23.54%	11.69%	0.38%	34.877	1.90	29.40%	70.60%
12	7-Jun-00	6:30 PM	3	1	0.00%	12.30%	22.70%	33.54%	28.64%	2.81%	5.083	0.37	12.30%	87.70%
13	10-Jun-00	11:30 AM	3	2	15.62%	54.30%	23.47%	5.57%	1.03%	0.00%	1.453	0.11	69.92%	30.08%
14	10-Jun-00	12:00 PM	3	1	41.29%	27.25%	12.84%	9.59%	8.23%	0.80%	40.408	2.95	68.54%	31.46%
17	14-Jun-00	3:30 PM	3	2	0.00%	60.68%	27.35%	8.55%	3.42%	0.00%	0.351	0.03	60.68%	39.32%
19	16-Jun-00	12:00 PM	5	2	61.84%	24.02%	8.32%	4.22%	1.52%	0.08%	221.754	4.88	85.86%	14.14%
21	16-Jun-00	2:45 PM	5	2	68.11%	16.50%	8.23%	4.75%	2.31%	0.09%	228.583	5.01	84.61%	15.39%
24	19-Jun-00	11:00 AM	3	1	0.00%	32.22%	25.37%	18.76%	22.08%	3.57%	1.786	0.13	32.22%	67.78%
34	21-Jun-00	10:00 AM	10	1	9.15%	22.62%	30.94%	27.93%	8.69%	0.67%	7.276	0.32	31.78%	68.22%
28	21-Jun-00	11:00 AM	5	1	73.06%	14.46%	6.49%	4.26%	1.67%	0.06%	275.843	12.10	87.52%	12.48%
30	21-Jun-00	2:40 PM	5	1	88.23%	4.04%	2.35%	3.13%	2.12%	0.14%	57.794	2.53	92.27%	7.73%
32	21-Jun-00	3:00 PM	10	1	12.06%	17.49%	16.18%	30.55%	22.12%	1.59%	13.978	0.31	29.56%	70.44%
31	21-Jun-00	3:25 PM	5	1	33.78%	26.94%	12.55%	14.64%	11.29%	0.79%	163.674	7.18	60.72%	39.28%
29	21-Jun-00	3:45 PM	5	1	27.84%	10.81%	5.35%	22.54%	31.49%	2.17%	12.574	0.55	38.45%	61.55%
36	23-Jun-00	11:30 AM	5	1	0.00%	8.77%	6.77%	19.87%	58.87%	9.73%	1.419	0.06	8.77%	93.23%
35	24-Jun-00	10:45 AM	5	2	31.37%	19.22%	12.56%	14.14%	19.28%	3.43%	177.703	7.79	50.58%	49.42%
38	26-Jun-00	10:40 AM	5	1	0.00%	3.73%	3.26%	23.14%	63.99%	5.87%	9.162	0.40	3.73%	96.27%
43	26-Jun-00	4:10 PM	5	1	34.61%	25.96%	17.03%	10.02%	10.46%	1.92%	743.676	32.62	60.56%	39.44%
41	29-Jun-00	10:00 AM	3	2	16.03%	27.34%	16.29%	18.40%	20.73%	1.20%	38.377	1.33	43.38%	56.62%
44	30-Jun-00	3:50 PM	5	1	41.15%	22.04%	9.80%	11.49%	14.03%	1.49%	87.195	3.82	63.18%	36.82%
46	1-Jul-00	6:20 PM	5	1	1.74%	5.24%	6.71%	22.08%	53.29%	10.95%	42.884	1.88	6.98%	93.02%
48	3-Jul-00	5:30 PM	5	1	16.12%	19.77%	14.40%	17.06%	29.29%	3.36%	24.843	1.09	35.89%	64.11%
47	3-Jul-00	6:45 PM	5	1	75.67%	2.04%	1.64%	4.33%	13.05%	3.27%	450.939	9.89	77.11%	22.29%
49	4-Jul-00	8:15 PM	5	1	1.92%	2.04%	2.29%	15.73%	67.01%	11.02%	197.279	8.65	3.96%	96.04%
51	6-Jul-00	6:10 PM	5	1	89.50%	1.02%	0.94%	2.86%	5.14%	0.54%	355.768	15.60	90.52%	9.48%
53	7-Jul-00	10:00 AM	5	1	0.86%	3.93%	4.48%	18.69%	63.50%	8.53%	30.147	1.32	4.79%	95.21%

Table 2-1. Little River bedload data.

Sample Number	Sample date	Sample time	Sample duration (min.)	Sample Location	-2.25 Phi (% by mass)	-1 Phi (% by mass)	0 Phi (% by mass)	1 Phi (% by mass)	2 Phi (% by mass)	3 Phi (% by mass)	Total sed. mass (grams)	FLUX (g/m.s)	% by mass gravel	% by mass sand
54	8-Jul-00	4:30 PM	7	1	71.76%	2.92%	1.38%	6.40%	15.54%	1.99%	1,139.678	35.70	74.69%	25.31%
70	10-Jul-00	1:14 PM	1	1	65.57%	6.73%	6.01%	10.10%	10.40%	1.19%	858.560	188.28	72.30%	27.70%
69	10-Jul-00	1:15 PM	5	1	35.13%	16.60%	15.42%	17.20%	14.24%	1.41%	312.902	823.43	51.73%	48.27%
67	10-Jul-00	1:20 PM	2	1	2.50%	3.77%	10.31%	40.67%	39.52%	3.03%	472.442	51.80	6.27%	93.73%
58	10-Jul-00	1:50 PM	3	1	72.34%	6.48%	5.31%	7.11%	7.13%	1.64%	690.393	50.47	78.82%	21.18%
66	10-Jul-00	1:56 PM	2	1	82.19%	4.79%	4.13%	4.48%	4.00%	0.41%	402.387	44.12	86.96%	13.02%
59	10-Jul-00	2:00 PM	5	1	31.63%	21.52%	2.94%	3.87%	32.51%	7.53%	1.938	0.08	53.15%	46.85%
65	10-Jul-00	2:00 PM	5	1	24.84%	22.95%	21.10%	17.17%	12.40%	1.54%	56.121	2.48	47.79%	52.21%
56	10-Jul-00	3:00 PM	3	1	31.29%	22.16%	4.90%	6.36%	30.40%	4.88%	29.038	2.12	53.46%	46.54%
71	10-Jul-00	4:40 PM	2	1	48.65%	17.52%	14.69%	12.89%	7.66%	0.59%	712.099	78.08	64.17%	35.83%
72	10-Jul-00	5:00 PM	2	1	6.95%	1.20%	4.87%	32.25%	48.89%	5.85%	342.619	37.57	8.15%	91.85%
73	11-Jul-00	1:15 PM	1	1	58.28%	12.55%	10.39%	10.94%	7.11%	0.73%	799.412	175.31	70.62%	29.18%
74	11-Jul-00	1:20 PM	2	1	11.92%	9.23%	17.92%	32.31%	25.64%	2.99%	730.867	80.14	21.15%	78.85%
76	13-Jul-00	1:10 PM	3	1	15.44%	16.82%	19.96%	27.09%	17.32%	1.37%	123.337	9.02	34.26%	65.74%
75	13-Jul-00	4:40 PM	3	1	53.78%	22.23%	13.33%	6.79%	3.33%	0.57%	1,354.003	98.98	75.98%	24.02%
78	15-Jul-00	12:50 PM	3	1	100.00%	0.00%	0.00%	0.00%	0.00%	0.00%	3,750.000	274.12	100.00%	0.00%
79	15-Jul-00	1:56 PM	3	1	100.00%	0.00%	0.00%	0.00%	0.00%	0.00%	7,100.000	519.01	100.00%	0.00%
61	19-Jul-00	1:40 PM	5	2	64.34%	14.82%	7.34%	7.44%	5.48%	0.58%	13.037	0.57	79.16%	20.84%
80	23-Jul-00	1:05 PM	5	1	100.00%	0.00%	0.00%	0.00%	0.00%	0.00%	6,600.000	289.47	100.00%	0.00%
64	23-Jul-00	2:20 PM	5	2	15.63%	41.12%	17.13%	13.09%	11.31%	1.72%	3.147	0.14	56.75%	43.25%
82	29-Jul-00	4:20 PM	5	2	37.53%	37.58%	15.62%	5.72%	3.27%	0.28%	6.506	0.29	75.12%	24.88%
83	2-Aug-00	12:00 PM	5	1	30.16%	8.31%	20.03%	48.95%	50.39%	4.48%	4.334	0.19	38.46%	121.85%

Table 2-1. Little River bedload data.

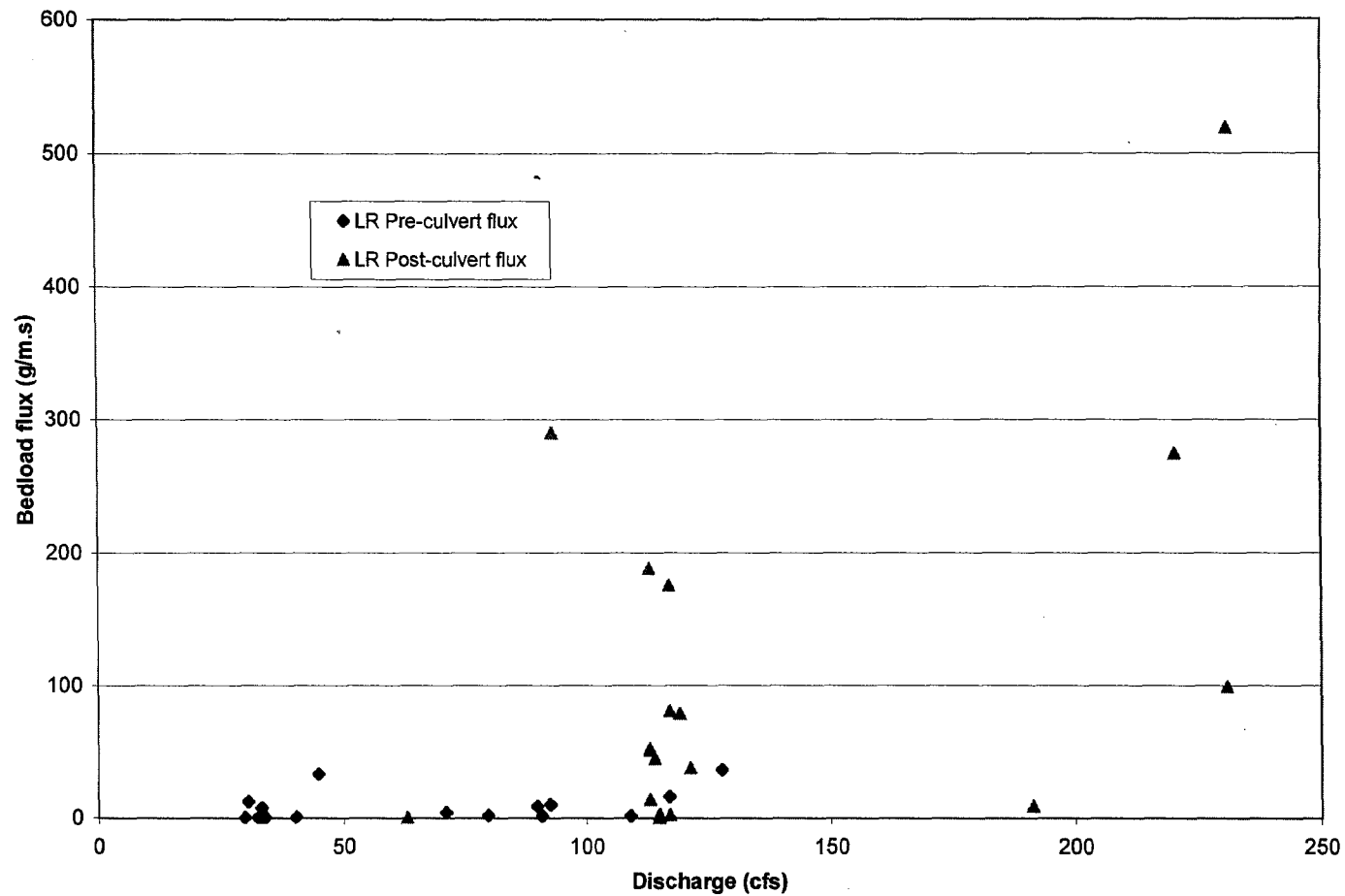


Figure 2-8. Little River Bedload rating curve measured at Cross-section.

Discussion

Prior to beginning field work, our initial working hypothesis was that the fluvial system, by definition, should be highly active, with much of the change in channel form during the melt season being due to the variability of discharge, sediment load, and characteristics inherent to braided streams. However, what we found was quite contrary to this premise.

Gravel-bar mobility

During the beginning of the melt season, when discharge was on the increase and activity should theoretically be increasing (as flow velocities and thus shear stresses exerted on the channel bed material), bedload movement was observed, on the order of $10^1 \text{ g m}^{-1} \text{ s}^{-1}$ (Figure 2-4, Figure 2-8, Table 2-1). Further, no significant changes in the location of gravel bars were seen, and no significant changes in channel cross section were observed. This does not imply that there was a complete absence of work being done on the system. On the contrary, there were localized occurrences of sediment movement, as smaller bars became axially flooded as the water surface increased. As these bars became flooded, the downstream facing slopes tended to be dissected as flow became channelized on the downslope face. As a result of this channelized flow, the fines in the bar material were winnowed away a short distance forming an apron, while the coarse material tended to locally collapse

in place, and not be moved a significant distance or become a large component of the sediment budget. To be sure, the changes noted were of small magnitude, and do not imply that the system ever tried to attain a new equilibrium more consistent with peak discharges.

Baselevel fall

As the melt season progressed and the existing culverts began to approach maximum discharge capacity, as a backwater pool began to form. This backwater pool, or pond (reservoir), grew larger as the discharge continued to increase while discharge capacity maintained constant. This had the effect of creating a level pool reservoir, with an energy slope approaching 0 (Figure 2-6b). Because the water is fully laden with silts and clays, where the energy slope (approximated by the water surface slope) intersects the channel banks, an identifiable “ring” of clay is deposited which marks the highest elevation of the backwater pool, as well as its upstream extent. This is extremely advantageous for analysis. It is evident that the clay ring profile projects to intersect the profile of July 10, almost exactly where the increase in slope occurs. As documented by Leopold and Bull (1979), results of channel impoundment (baselevel rise) lead to “wedges” of sediment building quickly. The sediment did not significantly continue to accumulate upstream past the height of the impoundment. Granted, their study charted the channel bed profile, and our study

tracks the energy slope changes, but parallels between the two parameters exist. As a result of LR's impoundment of flow by the culverts, a slug of coarse sediment was deposited in the backwater pool (Figure 2-9).

Upon removal of the original culvert design to avoid catastrophic failure, the backwater pool experienced a severe flushing episode. As a result of the greatly increased discharge capacity, the pond was able to drain, and the energy surface of the channel quickly increased its slope. Figure 2-6b shows that while the channel's energy slopes vary in elevation due to increases or decreases in overall discharge (see Figure 2-4), there is a zone of steep gradient increase at the upstream end of the clay ring. This indicates a small-scale, local, adjustment of slope by the stream to increase stream power, evacuating the stored sediment.

When the baselevel was nearly instantaneously dropped, the system responded with a hydraulic flushing of the accumulated clastic wedge. This is indicative of the stream attempting to restore its pre-impoundment grade, in the most efficient manner (Lai and Shen's "retrogressive erosion" [1996]). This efficiency is manifested in the channel cross-sectional widening, as it laterally erodes the loosely indurated material. Figure 2-7 shows the initial thalweg begin filled in with sediment, while the point bar become rapidly corraded laterally. In contrast, the active cut bar remained constant in geometry and experienced no corrasion or

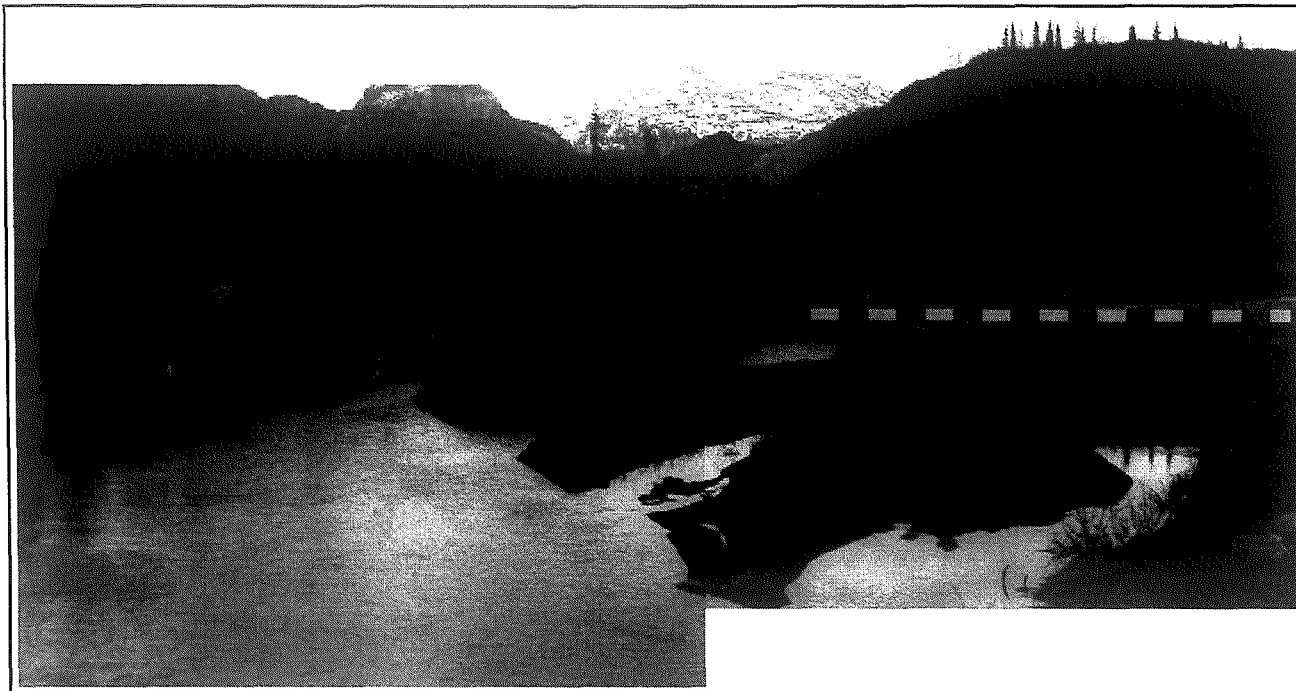


Figure 2-9. Shows the deposited clastic "wedge" upstream of culverts. Dashed line is cross section location from Figure 2-5. Flow is from upper right to lower left of page.

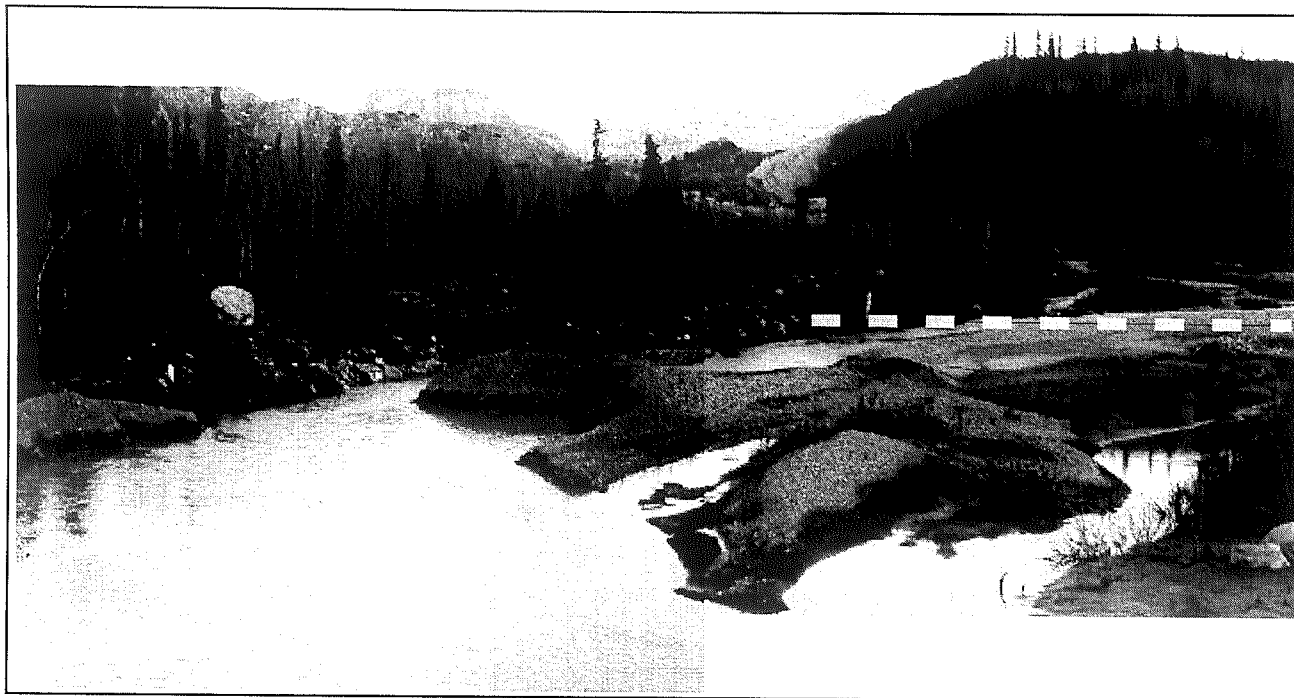


Figure 2-9. Shows the deposited clastic "wedge" upstream of culverts. Dashed line is cross section location from Figure 2-5. Flow is from upper right to lower left of page.

aggradation. Generally, the channel changed from relatively narrow and deep to wide and shallow. The cross channel profile line ends short of the section line, where no morphologic change had occurred. The small channel at the south end of the section line experienced flow for a period of days, when ponding was significant, but quickly emptied and never regained flow contribution after the culvert removal.

The initial thalweg aggraded, which indicates that sediment is being supplied to the channel. The channel widened in response to this influx of coarse sediment, because it increased the width to depth ratio of the channel, allowing for more efficient transport of coarse material for a given stream power - the discharge slope product (Leopold and Bull, 1979; cf. Bagnold, 1977). This is further supported by Ritter and Baker (1975), in that Bernoulli lift of particles is maximized in swift shallow flows, and is minimized in deep flows as the flow velocity vector at the channel bed becomes small. Also important to note is that the wave of erosion did not progress upstream of the deposited wedge of sediment, and where the stream profile was at initial grade (~150 meters easting in Figure 2-6b), no erosion took place.

A major contribution of this work is to provide insight as to the response rates and duration of the system as a result of the base level-fall. Schumm and Rea (1995) put forth the notion that fluvial systems behave as “damped springs”, with a

major response early, followed by an oscillating but overall exponential decay as the system approaches dynamic equilibrium. This is an attractive concept, and our documentation shows something quite similar.

Figure 2-10 shows the response of the system to the baselevel fall through time, measured as bedload flux, as well as magnitude of linear retreat of the major gravel bar (accumulated clastic wedge). The initial response occurs almost instantaneously, and is manifested as lateral corrasion. The summation curve shows the overall exponential decay of the response through time, supporting Schumm and Rea's 1995 theory that disturbed earth systems behave in this manner. A closer examination of Figure 2-10 reveals complex responses of the fluvial system to the baselevel fall – also seen in Schumm and Rea's (1995) experiments. The actual measured flux of sediment at first is low, but fluctuates to higher and higher proportions as the erosion of the bar wanes. There are two points where the transport and erosion curves cross over, possibly indicating which state of energy expenditure the system is in, and what process is dominating. For example, it is more efficient for the stream to first accommodate the increased energy gradient by increasing its cross-sectional area (widening), effectively lowering the discharge velocity. Then the system reaches a point where sediment being supplied to the channel is overwhelming, and the stream then switches its energy expenditure to removing the

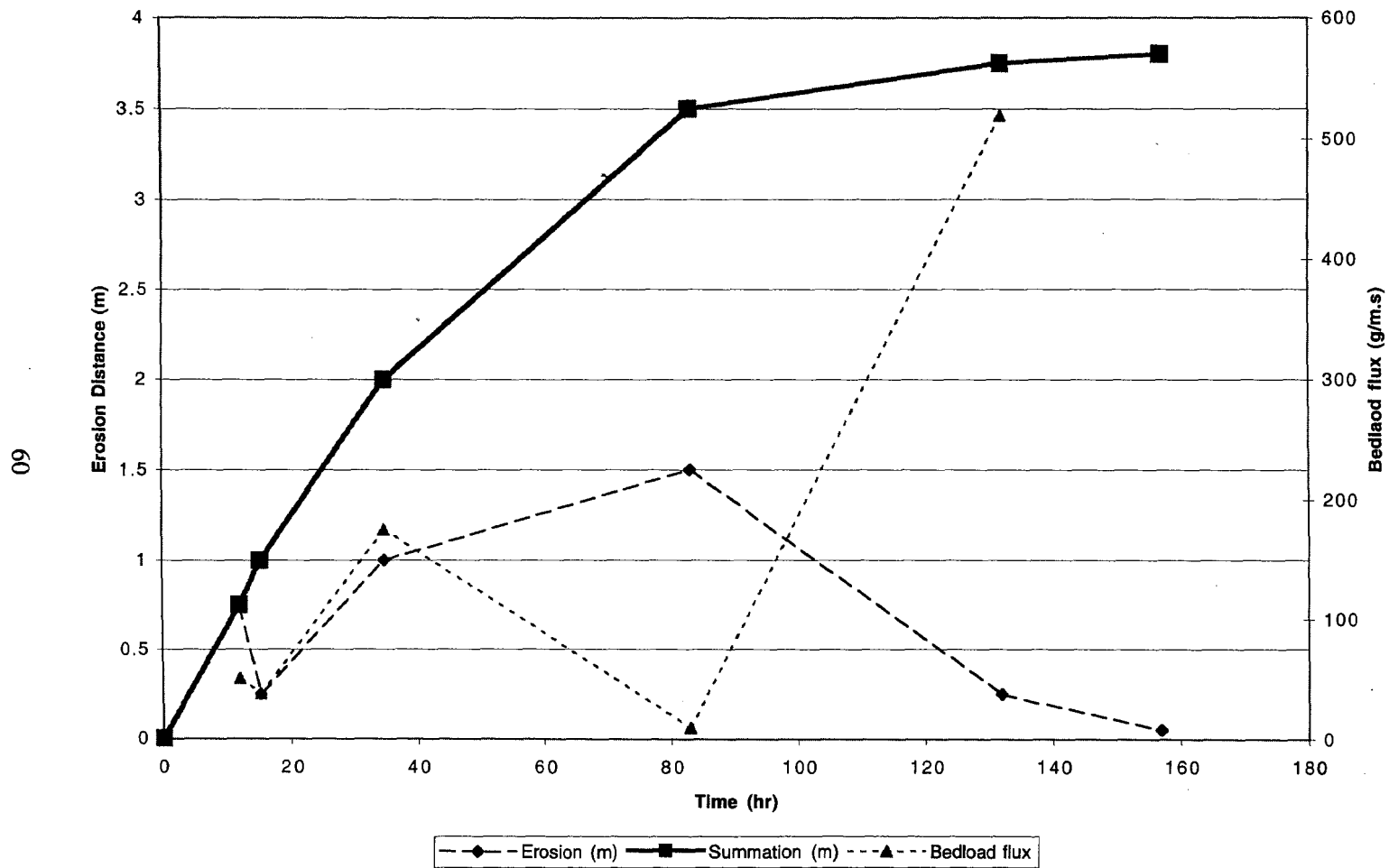


Figure 2-10. Magnitude of fluvial response through time.

excess amount of sediment being supplied to it. In other words, the system complexly oscillates alternately between sediment storage and sediment evacuation.

There are a few shortcomings with this analysis of the data. First, there is only one cross-section location. This at-a-station type data only provides information regarding the local reach, and cannot be considered as representative of the river's entire hydraulic geometry patterns (Leopold, Wolman, and Miller, 1964). Secondly, the diminishing of transported bedload toward hour 160 (Figure 2-9) may not necessarily represent true equilibrium of the system, rather it may simply be due to the falling discharge near this time (Figure 2-4). This implies that there is a definite discharge threshold for the system, below which sediment will not be entrained and evacuated. Finally, and related to the above point, we have only studied this system for one season. It would be enlightening to continue data collection next season, when the discharge hits peak flow, and the system continues to work itself towards a dynamically graded condition.

Conclusions

From the above discussion, we can conclude the following: Baselevel rise instigates accumulation of a clastic "wedge" as documented by Leopold and Bull (1979), and does not pass upstream of the point of break in energy surface slope.

Sudden local base-level fall stimulates a hydraulic flushing of the accumulated clastic sediments, and incision does not progress upstream of this point. The channel response is nearly instantaneous, and lasts for approximately 150 hours. Stream response is manifested by an increase in the width-to-depth ratio, characterized by lateral corrasion and local infilling of pre-existing thalweg. The nature of response times and rates are exponential decay and has complex responses of alternating sediment storage and evacuation.

References

- Alley, R.B., Cuffey, K.M., Evenson, E.B., Strasser, J.C., Lawson, D.E., Larson, G.E., (1997) How glaciers entrain and transport basal sediment: physical constraints. *Quaternary Science Reviews* **16**, 1017-1038.
- Bogen, J. (1996) Erosion rates and sediment yields of glaciers. *Annals of Glaciology* **22**, 48-52.
- ____ (1989) Glacial sediment production and development of hydro-electric power in glacierized areas. *Annals of Glaciology*, **13**, 6-11
- Chew, L.C. and Ashmore, P.E., (2001) Channel adjustment and a test of rational regime theory in a proglacial braided stream. *Geomorphology*, v. 37, p. 43-63
- Denner, J.C., Lawson, D.E., Larson, G.J., Evenson, E.B., Alley, R.B., Strasser, J.C., Kopczynski, S., (1999) Seasonal variability in hydrologic system response to intense rain events, Matanuska glacier, Alaska. *Annals of Glaciology* **28**,
- Evenson, E.B., Lawson, D.E., and 5 others (1999) Field evidence for the recognition of glaciohydrologic supercooling. *Geological Society of America special paper* **337**, 23-35.
- Germanoski, D. and Schumm, S.A., (1993) Changes in braided river morphology resulting from aggradation and degradation. *Journal of Geology*, v. 101, p. 451-466
- Gurnell, A.M. (1987) Suspended sediment. In *Glacio-fluvial Sediment Transfer: An Alpine Perspective*, eds. A.M. Gurnell and M.J. Clarke, Wiley, New York.
- Hallet, B., Hunter, L., and Bogen, J., (1996) Rates of erosion and sediment

- evacuation by glaciers; a review of field data and their implications. *Global and Planetary Change*, **12**, 135-213 ??
- Hunter, L.E., Powell, R.D., and Lawson, D.E. (1989) Morainal-bank sediment budgets and their influence on the stability of tidewater termini of valley glaciers entering Glacier Bay, Alaska, USA. *Annals of glaciology*, **13**, 211-216.
- Jaegar, J.M., Nittrouer, C.A., Scott, N.A., Milliman, J.D., (1998) Sediment accumulation along a glacially impacted coastline: north-east Gulf of Alaska. *Basin Research*, **10**, 155-173.
- Lai, J.S. and Shen, H.W., (1996) Flushing sediment through reservoirs. *Journal of Hydraulic Research*, v. 34, p. 237-255
- Lawson, D.E. (1993) Glaciohydrologic and glaciohydraulic effects on runoff and sediment yield in glacierized basins. *U.S. Army Corps Cold Regions Research and Engineering Laboratory Monograph: 93-2*, 107p.
- Leopold, L.B., and Bull, W.B., (1979) Base level, aggradation, and grade. *Proceedings of the American Philosophical Society*, v. 123, no. 3, p. 168-202
- Leopold, L.B., Wolman, M.G., Miller, J.P., (1964) Fluvial processes in geomorphology. W.H. Freeman and co. pubs., San Francisco, 522 pp.
- Milliman, J.D. and Syvitski, J.P.M., (1992) Geomorphic/tectonic controls of sediment discharge to the ocean: The importance of small mountainous rivers. *Journal of Geology*, **100**, 525-544.
- Oestrom, G. (1975) Sediment transport in glacial meltwater streams. In: A.V. Jopling and B.C. MacDonald (eds.), *Glaciofluvial and Glaciolacustrine Sedimentation. Society of Economic Paleontologists and Mineralogists – Special Publication. 23*, 101-122.
- Ritter, V.R., and Baker, D.F. (1975) Competence of rivers to transport coarse bedload material.. *Geological Society of America Bulletin*, v. 86, p. 975-978
- Schumm, S.A. and Rea, D.K., (1995) Sediment yield from disturbed earth systems. *Geology*, v. 23, p. 391-394
- _____ (1969) River metamorphosis. *Proceedings of the American Society of Civil Engineers*, v. 95, p. 255-273

Vita

Mr. Pearce was born in the western Chicago suburb of Oak Park, Illinois, on September 13, 1972, to Joan T. and Larry N. Pearce. He received his Bachelor of Arts in 1994 from Macalester College, St. Paul, Minnesota. After working in the GIS and hydrogeologic industry for 2 years including the USGS and National Park Service, Mr. Pearce enrolled at the University of New Mexico (Albuquerque) in order to pursue a MS degree in geology. During this time, he was actively involved with interdisciplinary research, ultimately being first author on two papers: *Evaporation in the Middle Rio Grande Bosque* and *G.I.S. analysis of Condensation Corrosion Residue in Lechuguilla Cave, NM*, both published in the Proceedings of ACE-PURSUE student conference (Jamshidi, Kaufmann, and Vadiee, eds.). He also was selected to collaborate with NSF-funded REU program with the Limnological Research Center at the University of Minnesota. Following the completion of academic deficiencies due to the change in discipline, Mr. Pearce was accepted to Lehigh University as a graduate student of fluvial geomorphology in the fall of 1999. While there, he was a teaching assistant of hydrogeology for 2 semesters, a teachers assistant for GIS and Computational Analysis for 1 semester, and a research assistant for 1 semester. He received his Master of Science degree in Geological Sciences in May 2001.

**END
OF
TITLE**